Energy Efficiency of Heterogeneous LTE Networks

HENRIK FORSSELL

KTH Electrical Engineering

Master's Degree Project
Stockholm, Sweden 2015

XR-EE-KT 2015:007

Abstract

Awareness of climate change and our environment is affecting the field of mobile communications. The challenge of reducing the carbon footprint and operating expenditures, while the demand for coverage and capacity is growing exponentially, is driving the trend of studying energy efficiency of mobile networks. Providing services in a resource efficient way have benefits both for the operator and the environment, which is why requirements on energy performance will be a part of the specifications of future 5G networks.

In long term evolution (LTE) networks, indoor small cells are deployed in large volume to improve performance in areas with poor macro coverage or high traffic demand. This type of network topology, that consists of several types of access nodes, is called a heterogeneous network (HetNet).

In this master thesis we study the energy efficiency of various HetNet deployments in a dense urban environment. The small cells deployments investigated are pico base stations and micro distributed-antenna-systems. Dense and sparse deployment strategies with varying transmit powers are compared. Furthermore, we investigate the potential for energy savings by setting the small cells into a low power sleep state under certain conditions. Both short sleep periods between transmissions, called discontineous transmission (DTX), and longer sleep cycles during periods of low activity is investigated.

This thesis was carried out as a project at Ericsson Systems & Technology in Kista, Stockholm 2015. To be able to evaluate the energy consumption at network level, realistic models for the power consumption of various base station types had to be implemented into a static radio network simulator.

Results show good performance of the considered HetNets but at a cost of higher power consumption than a macro only network. For example, a pico HetNet with twice the macro capacity consume 75% more energy over one day. However, results show that with DTX and sleep modes enabled, the daily energy consumption of the same HetNets is only 30% higher than the macro only network. Therefore, the main conclusion is that energy saving techniques will be of great importance for improving capacity without increasing network energy consumption.

Sammanfattning

Medvetenhet om klimatförändringar i vår miljö påverkar även utvecklingen av mobila kommunikationssystem. Att minska utsläppen av CO2 från kommunikationsindustrin samt minska operatörernas kostnader samtidigt som kraven på nätverkens kapacitet och täckning ökar är en utmaning. Denna utmaning driver en ny trend att studera energi-effektivitet i mobila nätverk. Att leverera tjänster på ett resurs-effektivt sätt är likväl lönsamt för operatörerna som för vår miljö. Detta är en anledning till att tydliga krav på nätverkens energiförbrukning nyligen har lagts till på listan över krav på framtida 5G nätverk. Basstationer med låg uteffekt, så kallade “small cells", är vanligt förekommande i dagens Long Term Evolution (LTE) nätverk. De placeras ut i områden med antingen dålig täckning eller höga krav på data trafik. Sådana nätverk, som består av flera typer av access-noder, kallas för heterogena nätverk. I detta projekt studeras energi-effektiviteten av heterogena LTE nätverk i tätbebyggd stadsmiljö. Access-noderna som studeras är så kallade Pico-noder samt olika “distributed-antenna -system". Flera olika nätverks-topplogier undersöks samt hur förändringar i access-nodernas ut-effekt påverkar energi-effektiviteten. Vidare studeras möjligheterna att spara energi genom att under vissa förutsättningar köra bas-stationer i ett läge av låg effektförbrukning. Dessa perioder kan variera i storleksordningen av en mikrosekund varvid det kallas “discontineous transmission", ända upp till flera timmar. De olika metoderna utvärderas med hjälp av ett statiskt simulerings-program för LTE nätverk. För att utvärdera energiförbrukning har realistiska modeller för bas-stationernas effektförbrukning implementerats i simulerings-programmet.

Acknowledgment

I would like to thank Dirk Gerstenberger and the people at Ericsson Systems & Technology for letting me carry out this project. Thanks to all of you who have been contributing with useful advice and interesting discussions! A special thanks to Gunther Auer who has been supervising the project.

I would also like to thank Tobias Oechtering who has been examining and supervising the project at KTH, and Erik Björkman who acted as opponent during the presentation of this thesis.

Contents

List of Figures

Acronyms

ADC analog-to-digital converter.

AI antenna interface.

BB baseband.

BS base station.

CSRS cell specific reference signal.

DAS distributed antenna system.

DL downlink.

DTX discontineous transmission.

EARTH Energy Aware Radio and netWork tecHnologies.

HetNet heterogeneous network.

LTE long term evolution.

MBSFN multicast and broadcast single frequency network.

OFDM orthogonal frequency division multiplexing.

OFDMA orthogonal frequency division multiple access.

PA power amplifier.

PDCCH physical downlink control channel.

PHBC physical broadcast channel.

PSS primary synchronization signal.

QoS quality of service.

RAN radio access network.

RF radio frequency.

SINAD signal-to-noise and distortion ratio.

SoTA state of the art.

SSS secondary synchronization signal.

TRX transmitter and receiver.

UE user equipment.

UL uplink.

Chapter 1

Introduction

1.1 Background and Motivation

The next-generation mobile networks are evolving in order to meet future needs on user experience and capacity. To meet the high traffic demand at indoor locations like office buildings, shopping malls and train stations, indoor small cells complementing the existing macro cellular network are being deployed in large volumes. At the same time, the energy efficiency of wireless networks has become increasingly important in recent years. It is therefore mandatory that these growing traffic demands will not result in an increased energy consumption of the mobile network.

Looking at the energy needed to operate a wireless mobile network, it is the base stations (BSs) that mainly contributes to the total consumption. Considering a mobile device, the major part of greenhouse-gas emissions during its life cycle comes from the manufacturing process. However, for a BS the opposite is true [17]. Also, mobile devices are already today very energy efficient since they need to be battery operated without frequent need of charging. A breakdown of the energy consumption of mobile networks show that 80% of the energy is consumed at the BS sites [6]. This justifies considering improvements in the BSs as the main contributors for a more energy efficient network.

Heterogeneous networks (HetNets), consisting of several types of BSs e.g. indoor small cells, can improve both the coverage and capacity of a traditional macro cellular deployment. However, from an energy efficiency perspective they can perform poorly since a large scale deployment of small cells together consume a substantial amount of energy. Additionally, small cells are not as frequently accessed as a large cell, which means that for most of the time they stand idle. Therefore, to improve the energy efficiency of HetNets, one can allow small cells to enter a low-power sleep-mode during idle periods. This strategy is expected to save energy particularly at low system loads, when the utilization of the small cells is low.

1.2 Problem Formulation and Method

In this work we have aimed to quantify as well as to improve the energy efficiency of various heterogeneous network topologies in a dense urban environment. The objective was to investigate how different network characteristics such as deployment strategy and type of small cells affect the energy consumption of the network. Furthermore, studies of how energy-saving technologies such as base station sleep modes and DTX can improve the energy efficiency have been carried out.

To study the behavior of dense urban LTE networks a static radio network simulation tool have been used. The simulation scenario is a 3D city designed to capture the characteristics of a Asian dense urban city. Propagation models in the simulator considers multi-path propagation and explicit walls and floors in buildings. Furthermore, traffic models allows for determining areas with higher traffic demand (HotZones). However, to be able to measure the energy consumption of the simulated network, power models for the different base stations had to be implemented into the existing simulation framework.

The energy savings fromDTX have been included as a statistical modification of the BS power models while longer sleep-mode periods are introduced by setting the transmit power to zero in the simulator. DTX and sleep modes have been simulated for various heterogeneous network topologies so as to be able to asses and compare the energy saving potential.

The objectives of the project were:

- Implement power models for different types of base stations into an existing radio access network (RAN) simulation tool.
- Evaluate the energy efficiency of the considered heterogeneous network deployments through simulations using the implemented power models. The energy efficiency will be measured under various network loads. The considered network loads range from busy hours with peak traffic demands to off-peak hours with extended cycles of idle traffic.
- Investigate how tuning the output power of the small cells affects the energy efficiency. With higher output power fewer small cells are needed since each cell covers a larger area.
- Assess the attainable energy savings of technologies that aim to improve the energy efficiency, such as DTX and base station sleep modes. Of particular interest are periods of low user activity where the highest potential for energy savings is expected.

While this study only considers a Asian dense urban simulation scenario, the implementations into the simulator allows for future studies of energy efficiency of LTE network deployments.

1.3 Previous Work

The Energy Aware Radio and netWork tecHnologies (EARTH) project was during the years 2010-2012 investigating the energy efficiency of mobile communication systems. The project was documented in a series of deliverables which, together with more information about the project can be found on the on the web-site [1]. There they state that:

"The goal of the project was to address the global environmental challenge by investigating and proposing effective mechanisms to drastically reduce energy wastage and improve energy efficiency of mobile broadband communication systems, without compromising users perceived quality of service and system capacity."

As a part of the EARTH project, mathematical models for the power consumption of various BS types were developed. These power models were used in simulations so as to be able to study the energy consumption at network level. Several types of deployment areas, e.g.rural, suburban, urban and dense urban were considered.

Linear power models for BSs is widely used for simulation studies of energy efficiency and energy savings. In [9] the energy consumption of HetNets consisting of macro and pico BSs are studied. Linear power models from the EARTH project are used in a generic 3rd generation partnership project (3GPP) simulation scenario were pico nodes are placed randomly within 100 m from each macro BS. Furthermore, in [16], the energy performance of LTE HetNets is studied in relation to the user experience by utilizing linear power models, again with a 3GPP simulation scenario.

In [18], different approaches to densifying urban networks are studied. Their simulation results show that indoor deployment of small cells is more energy efficient than densifying the macro deployment. The simulation scenario considered is a uniform "Manhattan-type city model".

DTX as an energy saving technique is proposed in [4] and the potential energy savings is studied in [3, 12, 7]. In [12] a DTX enabled macro deployment in a metropolitan area is studied through simulations.

The main contribution from this study is an assessment of the energy saving potential from the combination of short term DTX sleep and longer sleep modes specifically in the small cell BSs. Furthermore, the studied simulation scenario is more specific and detailed than the previous work we know of, considering a city with real buildings and realistic small cell deployment. The realistic 3D environment and specific site deployment in the simulator allows for ray-tracing propagation models that is more accurate than statistical models used in generic scenarios with random deployment.

1.4 Ethical Aspects

A study of the global carbon footprint of mobile communication [11] predicted an increase in $C0_2$ emissions by a factor of 3 in 2020 compared to 2007. According to this paper, information and communication technology (ICT) industry stands for 2% of the global $C0_2$ emissions which is higher than the emissions from global aviation. Mobile communication emissions constitutes about 25% of the emissions from the whole ICT sector.

Reduced energy consumption in mobile networks is a necessity to meet future requirements in a environmentally sustainable way. Furthermore, as mentioned earlier, reduced energy consumption also contributes to reduced operational expenditure for the network operators. Something that potentially could enable improvements of the communication infrastructure in developing countries.

1.5 Outline Of Thesis

The structure of the following chapters are as follows: In Chapter 2 we briefly describe basics of LTE HetNets with various types of indoor small cells. For later understanding of energy savings from cell DTX, we describe the downlink reference signals in LTE. In Chapter 3 we describe power consumption at BS level and various metrics for measuring energy consumption at network level. In Chapter 4 energy saving technologies are introduced with descriptions of how to model them in a simulation environment. Some notes on implementation aspects are included. Chapter 5 contains explanation of the simulation setup. In Chapter 6 the simulation results are presented with comparisons and discussion. Finally, in Chapter 7 conclusions are presented and future work is identified.

Chapter 2

Heterogeneous LTE Networks

A HetNet is a wireless network that consists of several types of access nodes. The access nodes, that can differ in terms of e.g. RAN technology or transmit power, provide non-regular coverage in a variety of area sizes. HetNets have shown to be an attractive solution for increasing the capacity of LTE networks [5] . In this section we describe the structure of LTE HetNets where the access nodes differ in terms of transmit power and size. We also provide a brief description of the LTE downlink physical layer since this is necessary for the understanding of discontinuous transmission (DTX) which is described in Section 4.1

2.1 Network Topology

Macro BS provide the baseline coverage of an LTE networks and these are generally deployed in groups of three sector-antennas which together form a BS site. The sites are usually deployed in a hexagonal grid with a coverage of 120 degrees per sector. Output power of a macro BS can vary between 5 and 40 W [8]. The inter-site-distance (ISD) is the distance between adjacent sites and can range from around 200 m in dense deployments up to several kilometers.

Since the efficiency of mobile network links is approaching the fundamental limits, network deployments need to be densified in order to meet the capacity requirements. With a sparse macro deployment the capacity can be increased by densifying the macro deployment itself. However, with already dense macro deployments, the gains from further densification is limited [8]. Also, high demand for capacity is often accumulated in certain highly populated areas called HotZones, e.g. train stations, shopping malls and office areas. In fact, 70% of all data traffic is served to indoor users [5]. Additionally, non-homogenous propagation environment caused by different types of buildings made from different type of material can cause coverage holes where the macro signal-strength is weak. These types of problems can be mitigated by deploying small cells.

Small cells are BSs with lower transmit power, ranging from 100 mW to 2 W, and therefore have a smaller coverage area than the macro cells. Small cells combat coverage holes and provide increased capacity in traffic HotZones. Depending on the transmit power and size of the coverage area, they are denoted micro, pico and femto BSs. Micro BSs have a range of less than 2 km. The range of a Pico BSs is shorter, less than 200m and femto BSs have the shortest range of around 10 m. Another solution is to use one radio unit that powers several antenna heads. This type of solution is called a distributed antenna system (DAS) [14].

2.1.1 Indoor Small Cells

Indoor areas can often suffer from poor macro coverage due to wall penetration losses. Additionally, the top floors of high-rise buildings can have particularly bad macro signal strength since macro sectors in urban areas are down tilted to better serve user equipments (UEs) on the streets. This makes indoor environment in urban areas a potential use case for small cell deployment. Another reason for considering indoor small cells is that high traffic demand usually is concentrated at indoor locations such as office buildings, train-stations and shopping malls.

For small cell indoor solutions, all different types of small cells can be deployed. However, Micro BSs are more often used in outdoor environment. Pico BSs can be useful in large office buildings, shops and other crowded areas, typically deployed on walls or in the roof. Femto BSs are more suitable for smaller rooms and are available as commercial home-solutions.

DAS is a typical indoor solution in office buildings. The antenna heads are connected via coaxial cables to a radio unit which corresponds to a macro or micro BS. The set of antenna heads connected to the same radio unit transmit the same radio signal together form a DAS cell.

2.2 LTE Basics

2.2.1 Orthogonal Frequency Division Multiplexing

Orthogonal frequency division multiplexing (OFDM) is a modulation technique where the transmitted signal consists of orthogonal sub-carriers in the frequency domain, see Figure 2.1.

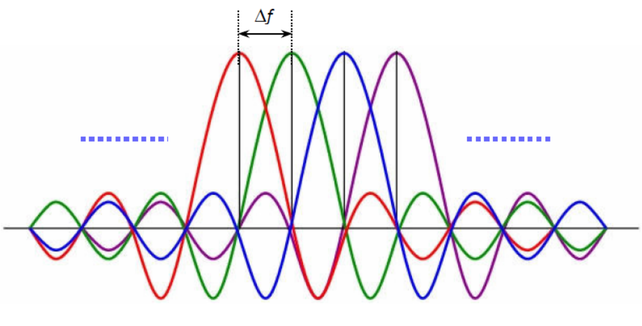

Figure 2.1: Orthogonal sub-carriers spaced by Δ_f in an OFDM modulated signal.

Due to the orthogonality of the sub-carriers, these can be independently modulated by a data symbol during one symbol duration. The transmitted signal during this symbol duration is defined as one OFDM symbol. The mapping of the data symbols to OFDM symbols is done by a serial-to-parallel converter followed by an inverse discrete Fourier transform (IDFT) after which the modulated signal is transmitted over the channel to the receiver. The receiver performs the inverse steps of the transmitter, i.e. a discrete Fourier transform (DFT) followed by a parallel-to-serial conversion, to recover the transmitted symbols. One benefit of OFDM is that it can transform a frequency selective channel into several frequency non-selective channels. As a result, channel equalization can easily be performed in the frequency domain and there is no need for complex time-domain equalizers. OFDM also benefits from utilizing the available bandwidth in a very efficient way [15].

2.2.2 Physical Layer

The downlink of an LTE system uses orthogonal frequency division multiple access (OFDMA). OFDMA let several different users to be scheduled on specific sub-carriers within an OFDM symbol. This makes it possible to dynamically schedule users both in time and frequency domain.

In time domain, the downlink (DL) signal is divided into fragments called radio frames of 10ms, each in turn divided into 10 sub-frames referred to as SF0-SF9. Every sub-frame is divided into 2 slots consisting of 6 or 7 OFDM symbols. The 20 time slots in a radio frame are the smallest resource element a user can be scheduled in time domain. The division of a radio frame into sub-frames and time-slots is depicted in Figure 2.2.

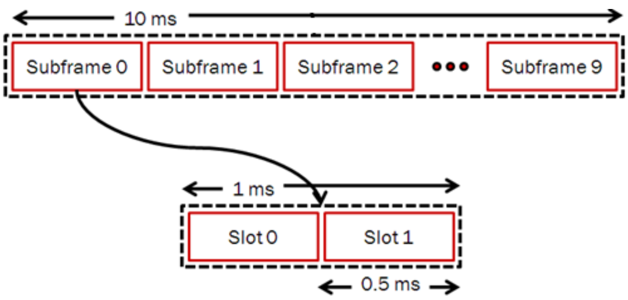

Figure 2.2: LTE radio frame in time domain divided into subframes and time slots.

In frequency domain, the DL signal consists of the OFDM sub-carriers which are spaced by 140 kHz. The numbers of sub-carriers depend on the bandwidth of the signal that can range from 1.4 MHz (72 sub-carriers) to 20 MHz (1200 sub-carriers). The smallest frequency domain element that can be scheduled to a user is called a resource block and consists of 12 OFDM sub-carriers.

Altogether, the smallest element that a user can be scheduled, called a physical resource block (PRB) or sometimes resource element (RE) consist of a time slot in time domain and a resource block in frequency domain as depicted in Figure 2.3.

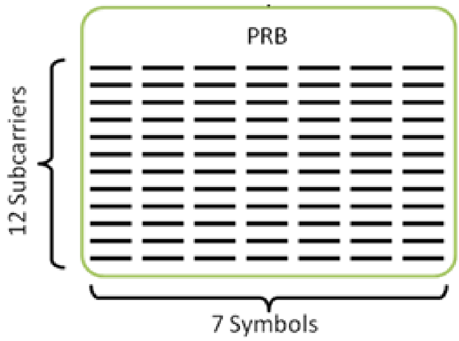

Figure 2.3: LTE physical resource block consiting of one time slot and 12 OFDM sub-carriers.

2.2.3 Reference Signals

From the DL signal, the receiving UE needs to be able to coherently demodulate the signal as well as identify the serving cell. Therefore, some of the REs in a radio frame contain cell-specific information that allows the UE to time-synchronize and estimate the channel conditions. This means that not all RE in a radio-frame carries user-specific data and even when a BS is not utilized, it still transmits these reference signals to idle subscribers.

For time-synchronization in LTE there is a primary synchronization signal (PSS) and a secondary synchronization signal (SSS) transmitted. Each radio frame contains two pairs of PSS and SSS signals located in OFDM symbol #5 and #6 of SF0 and SF5 illustrated by the blue and green regions in Figure 2.4. Each set of PSS and SSS is unique for the physical-layer cell ID (PCI) that identifies the serving cell. There exist 3 possible PSS sequences and 168 different SSS sequences which together make up a total of 504 unique PCIs.

There are cell specific reference signal (CSRS) within the individual sub-frames that allow the UEs to estimate the quality of the channel. In an ordinary sub-frame CRSs are located in OFDM symbols #0, 4 7 and 11 and these are illustrated as the violet regions in Figure 2.4. The CRSs are unique for all the 504 possible PCIs as well.

The users also need to demodulate information on what modulation and error correcting schemes that are used. For transmitting such information, there is a physical downlink control channel (PDCCH) in the beginning of each sub-frame, corresponding to the yellow regions in Figure 2.4. For broadcasting information to all users in the cell, there is aphysical broadcast channel (PHBC). This has resources allocated in four OFDM symbols in the second slot of SF0 corresponding to the red region in Figure 2.4.

As described above, the bandwidth of the OFDMA radio frame can be varied. The CSRS and PDCCH signals are then extended to fill the whole bandwidth. However, the PSS, SSS and PHBC are always allocated to the center 72 sub-carriers of the signal which can be seen in Figure 2.4. The rest of the REs in a radio-frame can carry user specific data.

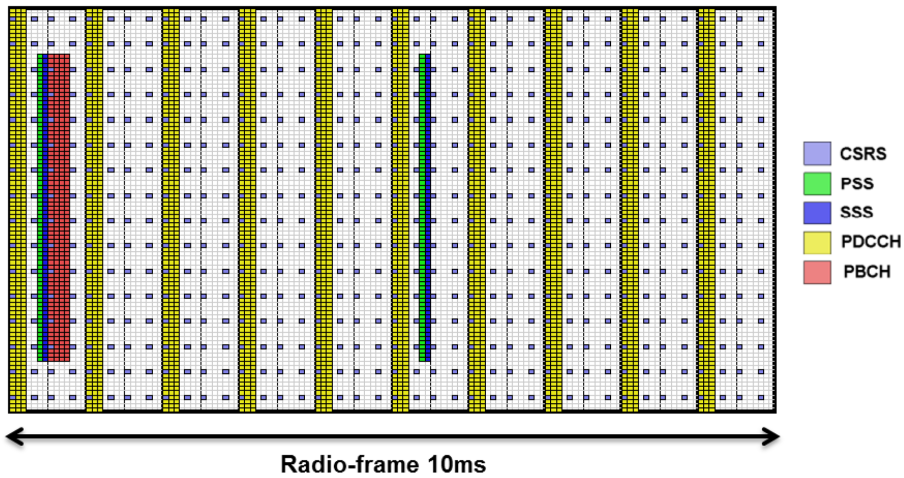

Figure 2.4: Location of reference signals in a LTE radio frame.

2.2.4 MBSFN Sub-Frames

In ordinary configuration of radio-frames CSRS are transmitted in every sub-frame. But since CSRS are cell-specific and a possible source of interference to neighboring cells, one may want to configure sub-frames without CSRS. Such sub-frames are referred to as multicast and broadcast single frequency network (MBSFN) sub-frames since they allow broadcasting of information, possibly from several BSs to UEs.

Depicted in Figure 2.5 is an LTE radio frame with the maximum number of MBSFN-subframes configured, i.e. SF2, 3, 4, 6, 7 and 8. If no users are scheduled, these six MBSFN sub-frame can be completely empty except for the PDCCH in the beginning [4].

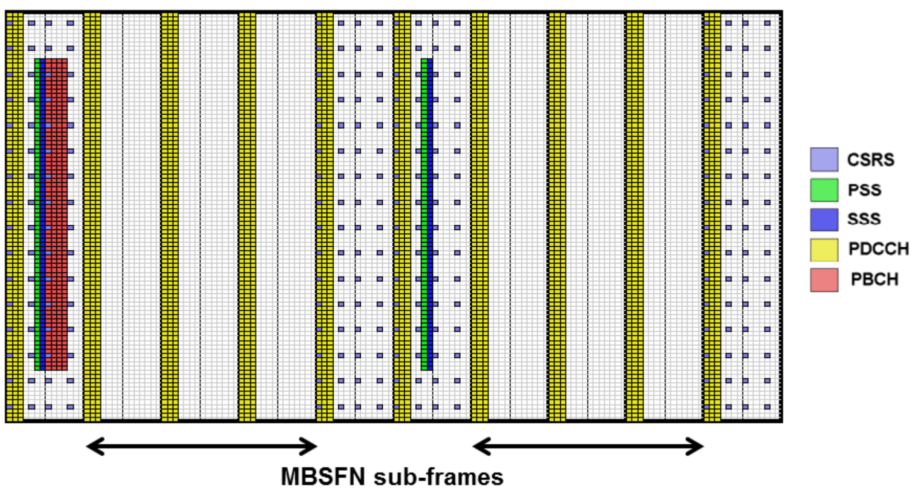

Figure 2.5: An LTE radio-frame with 6 MBSFN sub-frames configured.

2.2.5 Lean Carrier

Regular transmission of DL reference signals has its drawbacks. First of all, CRS and other cell-specific reference signals cause interference to neighbouring cells and can degrade the channel estimation of its cell-edge users. Secondly, unused reference signals give rise to uneccessary transmission energy. This effectively means that a BS that is not utilized but still transmits reference signals, both causes uneccessary energy consumption and interference in the network.

The idea of a new carrier type with reduced reference signalling is in [13] reffered to as Lean Carrier. For time synchronization and cell search in this setup, an extended synchronization signal (eSS) is proposed. In [13] they study the potential of Lean Carrier both in small cell and macro BSs and conclude that this technology can improve spectral efficiency and reduce energy consumption in HetNets.

Chapter 3

Energy Consumption of Mobile Networks

3.1 Energy Consumption Metrics

To quantify the energy consumption of mobile networks, metrics that relate the consumed energy to the coverage area and amount of transferred data are necessary. Designing a energy efficient network is a optimization problem that aims at minimizing the energy consumed by the network, while maintaining a specified quality of service (QoS). Therefore, it is important to consider the relation between energy consumption metrics and other performance quantities measuring the QoS. The typical behavior is that the energy consumption increase with the network load while the QoS experienced by the users decrease due to increased interference. The EARTH model defines two metrics, or energy consumption indices (ECIs) in [2]. These two are power per area unit and energy per bit and are described in detail in the following sections.

3.1.1 Power Per Area Unit

The power per area unit is denoted $ECI_{P/A}$. Due to the fact that the area covered by a particular deployment remains constant with varying traffic conditions, this metric is relevant for comparing different deployment scenarios. With the power supplied to the serving BSs denoted by P and the coverage area by A we can calculate

$$ECI_{P/A} = \frac{P}{A} \quad [\mathrm{W/m^2}]. \tag{3.1}$$

3.1.2 Energy Per Bit

The consumed energy per transmitted bit is denoted $ECI_{E/B}$. Denoting the number of useful data bits transferred by the system during a time period T by B and the total consumed energy by the same time period by E, we can calculate

$$ECI_{E/B} = \frac{E}{B} \quad [\mathrm{J/bit}]. \tag{3.2}$$

This can also be equivalently expressed in terms of the average supplied power $P = E/T$ and the average bitrate $R = B/T$ during the time period

$$ECI_{E/B} = \frac{P}{R} \quad [\mathrm{W/bit}/s]. \tag{3.3}$$

3.2 Base Station Power Models

The transmit power of the BSs, i.e. the power radiated from the transmit antennas, is an important parameter that affects the performance of wireless networks. However, designing an energy efficient network requires knowledge of the consumed power as well. Generally the consumed power in a BS is higher than the radiated power since other processes such as cooling and baseband signal processing consume a substantial amount of power. A power model is a mapping from the radiated power to the consumed power. As part of the EARTH project a state of the art (SoTA) BS power model was developed so as to be able to asses the energy consumption at system level. The breakdown of the power consumption of the modules in a BS and their load dependency showed that a linear power model is very accurate. See [2] for more details. As meantioned earlier, linear power models are frequently used in simulation studies of mobile network energy consumption, e.g. in [3, 9, 16, 18] models with similar parameters as in [2] are used.

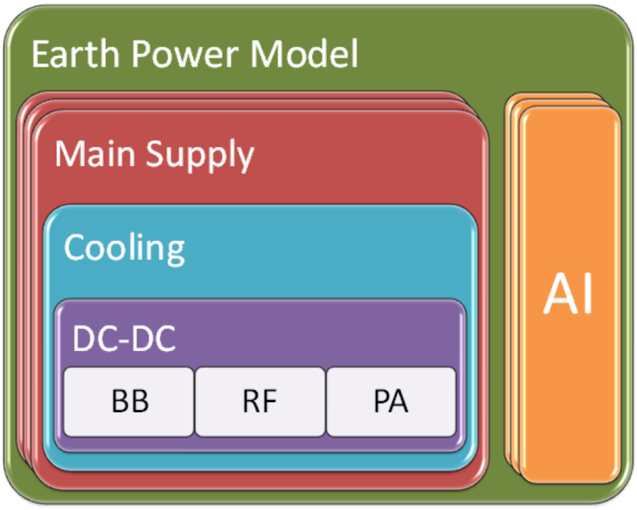

Figure 3.1: Power consuming modules in the EARTH SoTA power model.

Figure 3.1 depicts a typical structure that is applicable to all types of base stations considered in this report. A BS generally consists of several transmitter and receiver (TRX) modules. Each TRX module contain an antenna interface (AI), a power amplifier (PA), a radio frequency (RF) small signal module, a baseband (BB) engine, an active cooling system, a DC-DC power converter and a main power supply connected to the electrical power grid. The following section briefly explains the functionality of the different modules and how their power consumption depend on the load

- The **antenna interface** is the connection between the PA and the antenna. Here signals suffer from power losses due to feeders, filters and other components and is therefor relevant to consider in a power model. In remote radio head (RRH) units the PA is moved to the antenna location to limit the effect of feeder losses.

- The **power amplifier** in a BS normally suffers from poor power efficiency. This is because the PA is forced to work in a non-saturated regime to avoid non-linear distortions causing adjacent channel interference. In macro BSs, where the PA consumes a large portion of the power, digital techniques such as pre-distortion is used to improve the power efficiency. These methods are however not used in smaller BS types where the PA accounts for a smaller part of the power consumption.

- The **radio frequency** module is serving as analog-to-digital converter (ADC) for DL and uplink (UL) small-signals. Relevant factors for the RF power consumption are the required bandwidth, the allowable signal-to-noise and distortion ratio (SINAD), the resolution of the ADC and the number of antenna elements.

- The **baseband module** is a digital signal processor that performs the digital up- and down-conversion, OFDM modulation and other digital operations. It also constitutes the link to the backhaul network. The power consumption of the baseband module is mainly determined by the signal bandwidth, number of TX/RX antennas and which algorithms that the processor applies.

3.2.1 Load Dependency

The consumed power of the modules in a BS is more or less related to the load i.e. the amount of its resources that are utilized. Figure 4.1 show how the consumed power is distributed between the modules in different BS types. We can see that the percentage of the power consumed in the PA varies a lot between BS types e.g. 57% in a macro BS while only 35% in a pico BS. Furthermore, it is mainly the PA modules power consumption that is dependent on the load. This is due to the fact that decreased load results in non-occupied subcarriers and sub frames. The load variation in the other modules is very small and typically negligible compared to the PAs. As a result, the load dependency is very apparent in macro and micro BSs. While in low power BSs such as pico and femto, the power consumption is almost constant with varying load.

3.2.2 A Linear Power Model Approximation

The SoTA power models in [2] show a close to linear dependency between the BS load and the consumed power. This justifies the following model for the consumed power P_{in} of a BS with maximum output power $P_{\max}$ per TRX module.

$$P_{\text{in}} = N_{\text{TRX}}(P_0 + \Delta_p P_{\text{out}}) \,, \qquad 0 < P_{\text{out}} < P_{\max}. \tag{3.4}$$

Where N_{TRX} is the number of TRX modules, P_0 is the power consumption of one TRX module at zero load, Δ_p is the gradient modelling the load

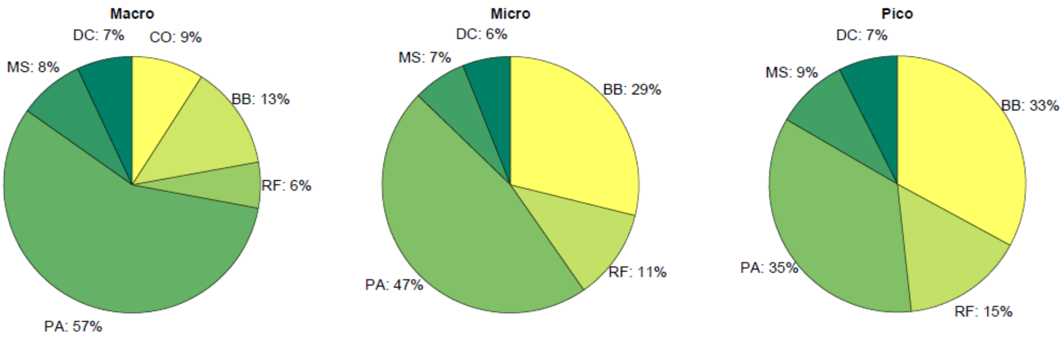

Figure 3.2: BSs distribution of power consumption between baseband (BB), radio frquency (RF), power amplifier (PA), main supply (MS) and DC-DC converter modules.

dependency and P_{out} is the output power. Additionally, with the definition of $u = P_{\text{out}}/P_{\text{max}}$, the consumed power can quivalently be expressed as

$$P_{\text{in}} = N_{\text{TRX}}(P_0 + \Delta_p P_{\text{max}} u) \ , \qquad 0 < u < 1. \tag{3.5}$$

The power models of macro, micro and pico BSs can be seen in Figure 3.3. The black line correspond to the power consumption of one macro sector, i.e. the power model in Equation (3.5) with $N_{\text{TRX}} = 2$. For one 3-sector macro site however, the power consumption is three times higher since this would consist of 6 TRX modules. The parameter values for the linear models of macro, micro and pico BSs can be seen in Table 3.1. These parameters are from [2] and have been determined by least squares fitting this linear model to the data from the SoTA power model.

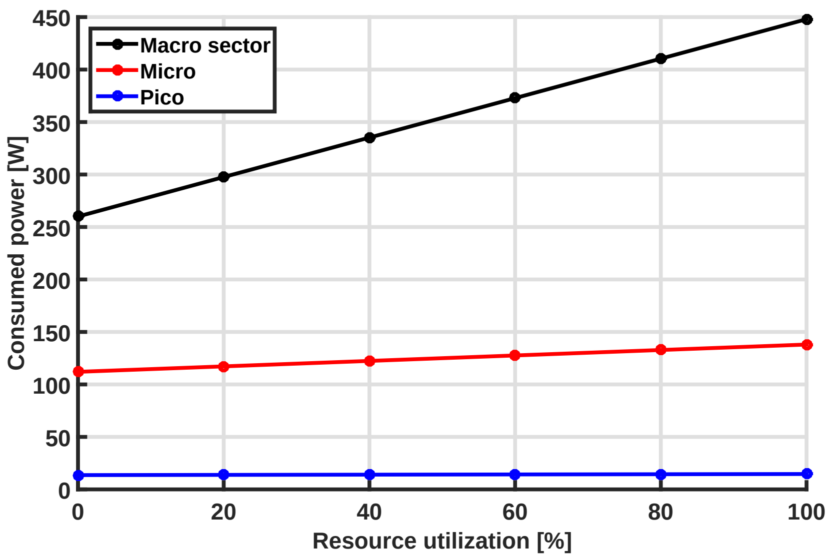

Figure 3.3: Linear power models for macro sector, micro and pico BSs.

Table 3.1: Linear model parameters for different BS types

BS Tyoe	N_{TRX}	$P_{\max}$ [W]	P_0 [W]	Δ_p	P_{sleep} [W]
Macro	6	20.0	130.0	4.7	75.0
Micro	2	6.3	56.0	2.6	39.0
Pico	2	0.13	6.8	4.0	4.3

3.2.3 Average Power Consumption Model

The power model described by Equation (3.5) maps the instantaneous utilization u of the PA to the instantaneous power consumption P_{in}. However, generally the instantaneous utilization is a function of time $u(t)$ that varies rapidly with the traffic on a short time scale [10]. Which means that the instantaneous power consumption is also a function of time $P_{\text{in}}(t)$.

In the static simulator used in this work, which will be further described in following chapters, the output only contains the average utilization over a time interval $t \in [0, T)$. Here we will show that applying the power model before or after the averaging yields the same average power, i.e applying the power model to the output of the simulator is justified. The average utilization is defined as

$$\bar{u}_T = \frac{1}{T} \int_0^T u(t) dt \tag{3.6}$$

and the average power consumption over the same interval is

$$\bar{P}_T = \frac{1}{T} \int_0^T P_{\text{in}}(t) dt. \tag{3.7}$$

If we now apply power model (3.5) into (3.7) we get

$$\begin{aligned} \bar{P}_T &= \frac{1}{T} \int_0^T N_{\text{TRX}}(P_0 + \Delta_p P_{\max} u(t)) dt \\ &= N_{\text{TRX}} \left(P_0 + \Delta_p P_{\max} \frac{1}{T} \int_0^T u(t) dt \right) \\ &= N_{\text{TRX}}(P_0 + \Delta_p P_{\max} \bar{u}_T). \end{aligned} \tag{3.8}$$

since integration and summation can be interchange and due to the fact that the constant term $N_{\text{TRX}} P_0$ does not depend on t. From Equation (3.8) we can conclude that we can calculate the average power consumption $\bar{P}_T$ by applying the power model to the average utilization $\bar{u}_T$. In addition, we should emphasize that this result only holds as long as the power model is linear.

Chapter 4

Energy Saving Technologies

4.1 Cell Discontineous Transmission

Increased battery life in mobile devices has for a long time been an attractive feature and a selling-point for manufacturers. The fact that UEs does not receive and transmit data all the time can be exploited for energy savings by using (DTX), a well-known feature used in mobile devices [10]. It allows the transmitter to go into a low-power state during periods of low activity, only to wake up for short periods of time to check for pending data transmissions.

Studies show that BS traffic is bursty on a short time scale as well. This fact makes potential for energy savings in BS by putting the PA into sleep for periods of no transmissions, called cell DTX.

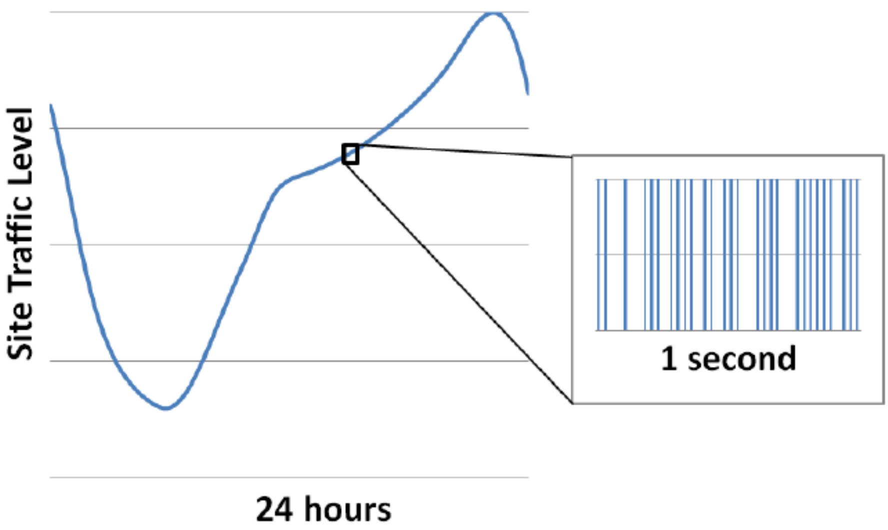

Figure 4.1: Daily BS traffic pattern on long and short time-scale.

However, cell DTX gives rise to new challenges that are not present on the UE side. Firstly, since the BS needs to schedule several transmissions to different UEs, the problem of determining when to put the PA into sleep is much more complex. Secondly, even when there are no transmissions scheduled, the UEs rely on the continuous transmission of radio frame control signals (see Subsection 2.2.3) to be able to connect and synchronize to the BS. But with the configuration of MBSFN sub-frames or possibly lean carrier design (see Subsection 2.2.4) it is possible to reduce the amount of reference signaling in a radio frame without degrading performance. This does not only contribute to increased energy efficiency but also decreased interference, since some reference signaling is removed (source). Cell DTX can be configured on different time scales ranging from OFDM symbol level to radio-frames.

Powering up the PA from sleep takes a certain wake-up time T_{w}. In [12] $T_{\text{w}} = 30\mu s$ wake-up time is assumed and that putting the PA into sleep is instantaneous. This can be compared with the duration of one OFDM symbol

$$T_{\text{OFDM}} = \frac{T_{\text{subframe}}}{N} = \frac{1}{14}[\text{ms}] \approx 71\mu\text{s} \tag{4.1}$$

to conclude that the wake up time is in the order of one half ODFM symbol. However, modern hardware will most probably be able to support PA wake-up times down to 10 μs.

The difference between possible configurations for LTE are described in the following sections. One can also consider longer sleep periods e.g. several hours, with this type of configuration it is called sleep modes. This is described in Section 4.2.

4.1.1 Micro DTX

In Subsection 2.2.3 the structure of an ordinary LTE radio-frame is described. In this structure, all the sub-frames contain CSRS, but these signals are only transmitted in some of the OFDM symbols. If this structure is kept, we are limited to allow PA sleep on the empty OFDM symbols of the LTE radio-frame. This is the DTX configuration on the shortest time scale, called micro DTX.

With this configuration, assuming the maximal amount of 3 OFDM symbols used for PDCCH and that no users are scheduled, the PA can be in sleep mode during 73 of the 140 OFDM symbols with a resulting 37 number of wake up events. Assuming the $10\mu s$ wake up time, this allows 4.1 ms of sleep during one radio frame which corresponds to 41% of the time

4.1.2 DTX With MBSFN Sub-Frames

If the possibility of configuring MBSFN sub-frames is utilized, we can allow longer DTX cycles in some of the sub-frames. However, the PA still needs to wake up for the 3 OFDM symbols containing the downlink control region in the beginning of the MBSFN sub-frame.

In this configuration, with the same assumptions as in Subsection 4.1.1, we find that the duration that we can allow the PA to be in sleep mode is increased to 91 OFDM symbols with only 19 wake-up events. This yields a total 5.9 ms (59%) of effective sleep during one radio-frame.

4.1.3 DTX With Lean Carrier

It is clear from the configuration of the LTE radio-frame that it is mainly the CSRS and PDCCH that are preventing the PA from going to sleep. If we consider a lean carrier design as described in Subsection 2.2.5, it would be possible to increase the the fraction of sleep at zero load up to almost 100%.

4.1.4 Average Power Consumption with DTX

By utilizing DTX, the average power consumption can be reduced. The average resource utilization $\bar{u}_T$ can be thought of as the probability that a user is scheduled on a PRB. Denote the power consumption of the PA in sleep mode P_{sleep}.

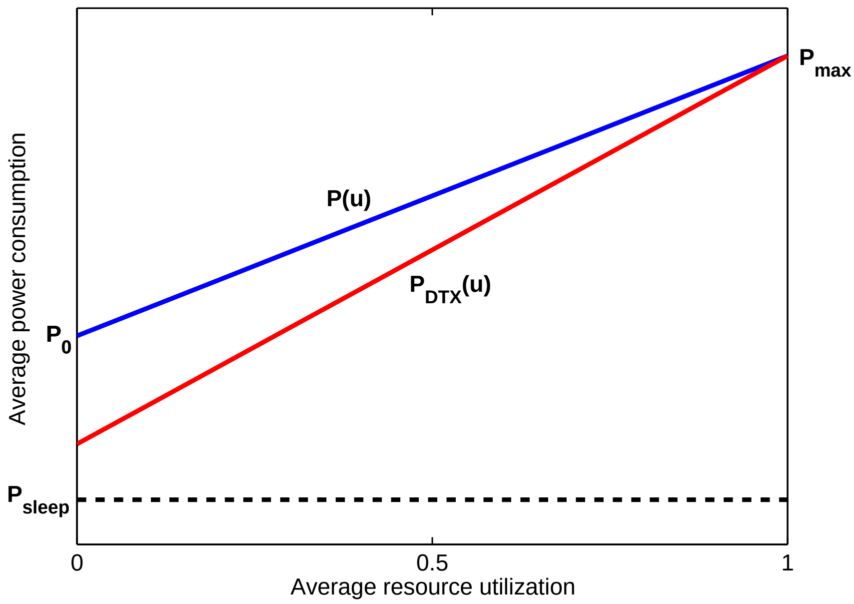

Figure 4.2: Modification of power model to account for cell DTX energy savings.

The average power consumption of the BS without DTX

$$\bar{P} = P_{\text{model}}(\bar{u}) \tag{4.2}$$

is a function $P_{\text{model}}(.)$ of the average utilization given by 3.8. With the definition

$$\tau = \frac{T_0}{T_{\text{radioframe}}} \tag{4.3}$$

where $T_{\text{radioframe}}$ is the duration of one radio-frame and T_0 is the total duration of effective sleep during a radio-frame with no users scheduled, the average power consumption for a given average resource utilization can be calculated as

$$\bar{P}_{\text{DTX}} = \tau(1-\bar{u})P_{\text{sleep}} + (1-\tau(1-\bar{u}))P_{\text{model}}(\bar{u}) \tag{4.4}$$

4.2 Small Cell Sleep Modes

Considering the power models in Section 3.2, one macro BS approximately corresponds to 10 pico BS in terms of power consumption. The relatively low power consumption of the small cells makes them interesting from an energy-efficiency perspective, however, the small coverage-areas generally makes need for large scale deployment which can make the total power consumption of the small cell layer high. Nevertheless, low power consumption together with a high amount of served traffic in HotZones results in a high energy-efficiency in terms of energy per bit. Because of this, networks in dense urban areas with traffic HotZones can benefit from small cell deployment both in terms of QoS and energy-efficiency when there is high activity in the HotZones [3].

The fact that small cell BSs have an almost constant power consumption at variable load makes potential for energy savings when a node is not utilized. In such situations, switching off or putting the BS in a low power sleep can save energy at network level while still maintaining the same QoS. When to put small cells into sleep can either be controlled by some sort of central network algorithm, or by a distributed algorithm consisting of decisions in the small cells.

Small cells in HetNets are typically deployed for two reasons, either to increase signal strength in areas where the macro coverage is weak, or to increase capacity in traffic HotZones. In the first scenario, a distributed algorithm can be problematic since this will introduce coverage holes for potential UE entering the cell. In the latter case however, since the UEs have macro coverage, a centralized decision whether to switch on the small cell is possible.

It would be possible to have a distributed algorithm that keeps the cell in idle mode for a certain amount of time before going to sleep. The problem that arises is how to know when to switch on the cell again. One solution would be to introduce a low power sniffer with a threshold on received signal power. This way users entering the small cell could be detected.

Chapter 5

Simulations

5.1 Static RAN Simulator

In order to evaluate the energy efficiency of a heterogeneous network deployment we have used a static RAN simulator. The simulations considers a 3 dimensional area with fixed BS and UE positions. Each UE is connected to a BS which handles both UL and DL traffic. In the static simulator the propagation environment is determined either by ray-tracing or statistical models and interference from other nodes is also considered. After this statistical short-term traffic models are applied to estimate the performance of the links in the network. In this chapter we briefly explain the propagation and traffic models that were used in the simulations. Additionally, to asses the energy consumption on a longer time scale, long-term traffic models that model the traffic behavior during one day are needed, these are described in this chapter as well. Finally the simulation scenario with map, deployment and various simulation parameters are introduced.

5.2 3D Map and User Deployment

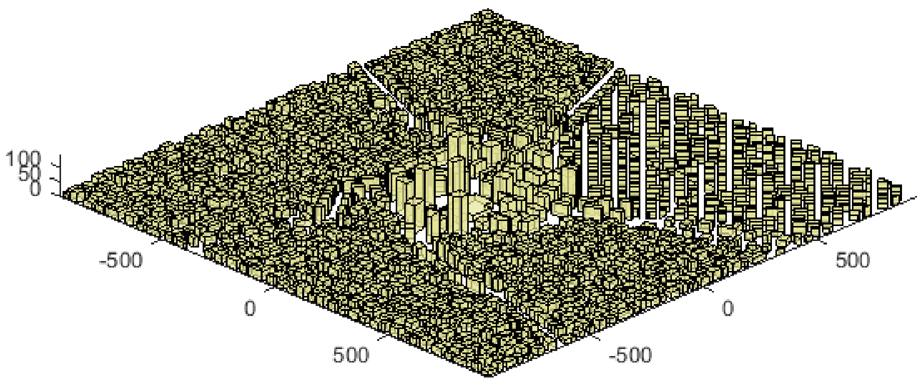

Figure 5.1: Map of simulation map with central area marked in grey

The simulated environment is built up by 2-dimensional square bins which in this work have the dimension of 5x5 m. The map is vector based and contains buildings of different heights and footprints. Different bin-codes describe the location and type of the bins e.g. indoor, outdoor, street and HotZone. At building locations several bins are stacked on top of each other for every floor of the building. UE nodes are deployed in a fraction of the bins, e.g. every second bin. This map sampling only considers the 2-dimensional area which means that the user density (from 2-dimensional perspective) will be higher at building locations.

5.3 Propagation and Traffic Models

In the static simulator, the propagation environment needs to be determined. This is done either with statistical models or ray-tracing. All the simulation results in this work is simulated using a ray-tracing propagation model called BEZT. BEZT models multi path propagation from the transmitters to the receivers and finds the channel gain for each path. The channel gains over all the links are stored in a large matrix which is used to calculate the received signal quality in every receiver.

5.3.1 Short-Term Traffic Model

From the propagation and interference modeling the signal-to-interference-and-noise-ratio (SINR) for each link is known. This can be mapped to an available link bitrate based on the modulation scheme that is used. The available link bitrate is the throughput the user would experience if the link was utilized all the time. However, in real networks the links are not constantly utilized. Instead, file downloads happen randomly according to some distribution which can be captured by a statistical traffic model.

The simulator uses an equal buffer traffic model to simulate file downloads and estimate the experienced user throughput. In the equal buffer model, all user sessions are of a fixed file-size. The sessions arrive according to a Poisson process and the users fully utilize the available link bitrate during a file download. The areal traffic is specified in terms of offered traffic as e.g. traffic per bin or traffic per m^2. This offered traffic is due to capacity limitations of the deployed network not always possible to serve to the users which results in a total served traffic which is always lower than the offered traffic.

In order to evaluate how different results depend on the traffic load, several simulations are performed with varying amounts of offered traffic. However, to compare performance between several simulated networks we plot them against the served traffic.

5.3.2 Long-Term Traffic Model

As described above, the static simulator can capture the performance of the network by modeling the dynamic traffic with statistical models. This results in a snapshot of the network during a short time period where the average traffic behavior i.e. total amount of served traffic remains constant. However, in real networks the traffic behavior of course varies on a long time scale as well e.g.

low amount of served traffic during night hours etc. To map the performance from the short-term static simulations to long-term results we in this work apply a daily traffic profile with an hourly resolution.

The daily traffic profile from [2] is the results of measurements in a real LTE network in Europe. The traffic profile in terms of percentage of peak area throughput is depicted in Figure 5.2. While peak throughput varies between areas, e.g. urban areas has higher peak throughput than rural areas, the envelope of the traffic profile in Figure 5.2 is applicable to all types of areas.

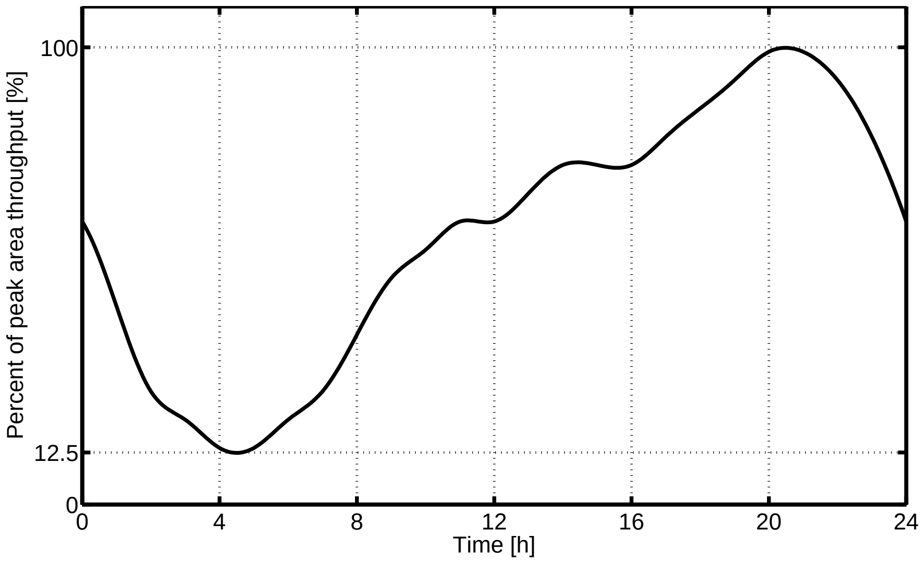

Figure 5.2: Daily traffic model in percentage of peak area throughput.

We consider a daily traffic profile to be able to map it to a daily energy consumption. The steps of this process, which was developed during this thesis project, are the following:

- Peak area throughput in terms of Mbps/m^2 is specified. This quantity is the traffic load at the peak hour in the daily traffic profile.
- A 4th degree polynomial is least square fitted to the simulated power consumption for different traffic loads, i.e. served traffic. An example of such a function with corresponding data points can be seen in the upper left part of Figure 5.3.
- The polynomial function is then used to map the hourly served traffic to an hourly power consumption which is illustrated by the dashed lines in Figure 5.3.
- A sum over the hourly power consumption then calculates the daily energy consumption.

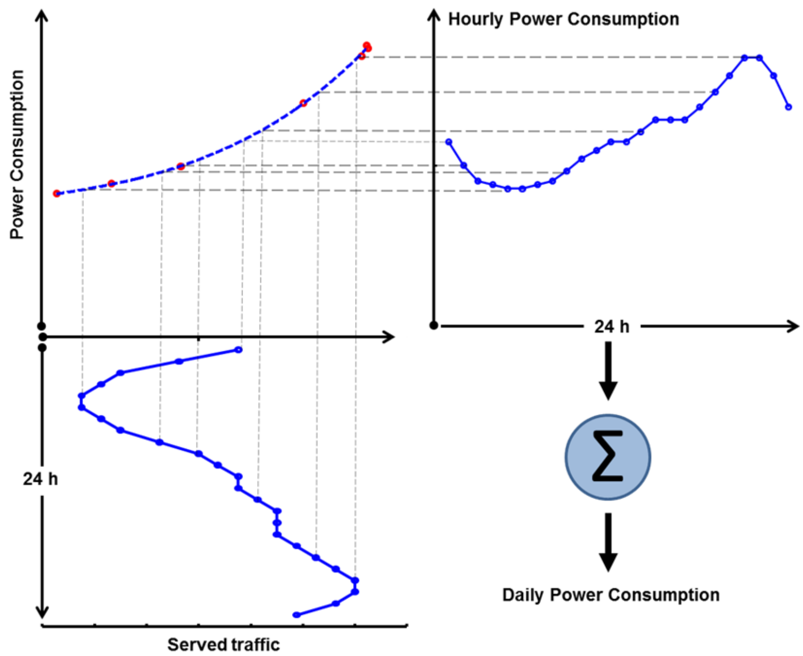

Figure 5.3: Process of mapping simulation results to daily power consumption.

5.4 Simulation Scenario

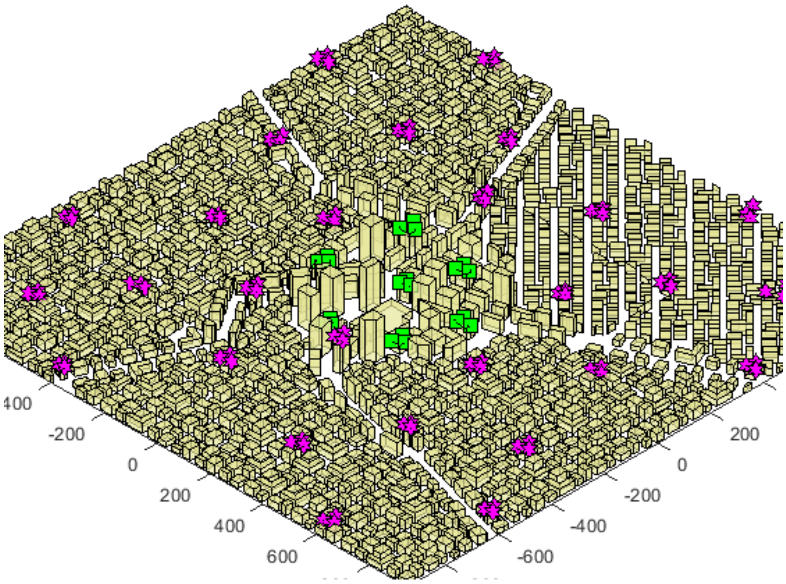

Figure 5.4: Close view of macro deplyment in the 3D map.

The scenario considered is a model of a dense Asian city inspired by Tokyo and Seoul. The map, which is depicted in Figure 5.1 consists of a 1000x1000 m central area with high-rise buildings surrounded by a dense urban area. A close view of the macro deployment in and around the central area can be seen in Figure 5.4. In the center of the map a dense layer of 7 macro sites is deployed with ISD = 200 m. These nodes are referred to as the center macro layer and correspond to the green squares in Figure 5.4. Around the center an additional 28 macro sites with ISD = 400 m are deployed. These correspond to the purple stars in Figure 5.4 and are referred to as the surrounding macro layer. This map and macro deployment was kept throughout all simulations. Table 5.1 summarizes the most relevant simulation parameters which were kept throughout all simulations.

Table 5.1: Simulation parameters

Parameter	**Value**
System	Uplink and downlink FDD with 10 MHz per carrier
Carrier frequency	2 GHz
Modulation scheme	4, 16 and 64 QAM
Macro deployment	Capacity macro layer: 7 three-sector sites with ISD = 200 m Coverage macro layer: 7 three -sector sites with ISD = 400 m
Macro TX power	40 W/sector
Propagation model	BEZT
Traffic model	Equal buffer

5.4.1 Indoor Deployment

- **Indoor deployment #1** have a sparse deployment of small cells in the 10 largest buildings in the central area. The office coverage area is 1000 m^2 per node and the placement of the nodes is depicted in Figure 5.5.

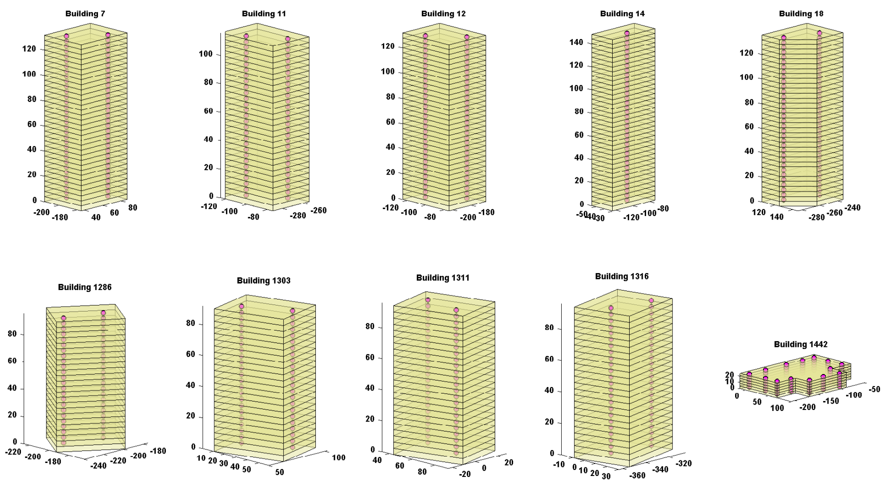

Figure 5.5: Sparse small-cell deployment in 10 largest buildings.

- **Indoor deployment #2** have a dense deployment small cells in same 10 buildings. The office coverage area is 600 m^2 per node and the placement of the small cells can be seen in Figure 5.6.

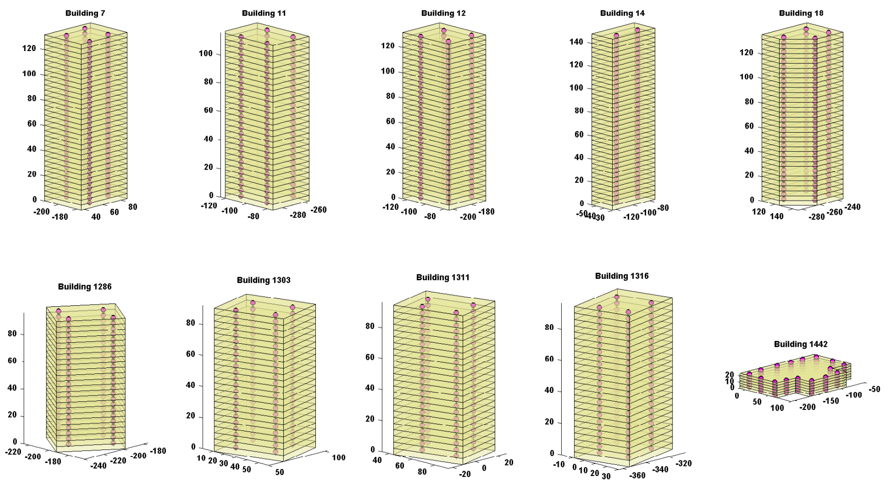

Figure 5.6: Dense small-cell deployment in 10 largest buildings.

The deployment scenarios determine the placement of the nodes. Pico nodes with variable transmit power and DAS with various number of antenna heads per cell are considered. The system parameters for the different access nodes can be seen in Table 5.2

Table 5.2: Small Cell System Parameters

Pico	
Tx power	100mW, 200mW and 500mW
N Tx/Rx antennas	2
Micro DAS	
Transmit power	10 W
Number of antennaheads per cell	4, 8 and 12
Feeder loss	10 dB

5.4.2 Traffic

The traffic demand is specified per m^2 for different area types. In real networks traffic is normally heavier at indoor locations due to higher user density. This is captured in the simulations by defining 80% of the traffic to indoor bins and 20% to outdoor bins. This specification considers office area, i.e the area over which the indoor traffic is distributed is considering all floors in all the buildings. Additionally, HotZones are specified in the 10 buildings with small cell deployments. Figure 5.7(a) show the traffic zones with no HotZones specified and 5.7(b) show the 10 building HotZones. The fraction between traffic demand in the 10 HotZone areas and the rest of the buildings can be set in the simulations.

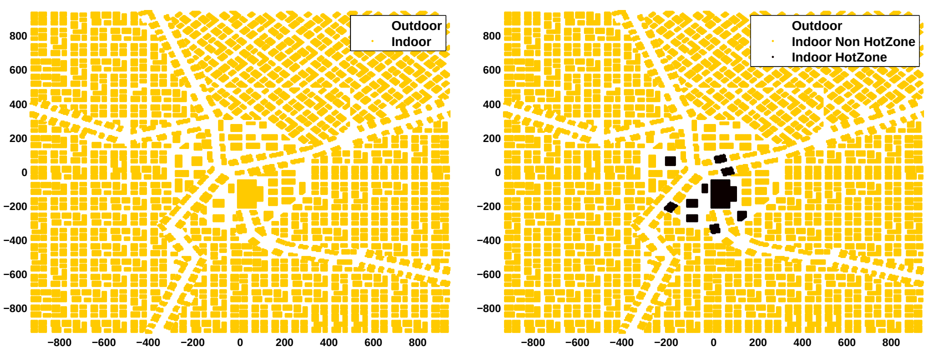

(a) Uniform

(b) Indoor HotZones

Figure 5.7: Spatial traffic distributions illustrated in map. Compare (a), where the traffic is uniformly distributed in all indoor area, with (b) where there are traffic HotZones in the 10 largest buildings.

5.4.3 Power Models and Energy Saving Technologies

The specific power models used in the simulations can be seen in Figure 5.8. This figure also includes the effective power model when considering energy savings from DTX. In 5.8(a) the macro power model for one sector is shown and the DTX scheme considered is Micro DTX. In 5.8(b) the power models for 100 mW and 500 mW pico nodes is plotted. In the pico nodes we consider three energy saving schemes namely Micro, MBSFN and Lean Carrier DTX.

The power model for a DAS cell is the same as for one micro BS. The feeder losses of the DAS cells affects the output power from the antenna heads, e.g. introducing more antennas per cell decreases the output power from each head. However, the output power from the radio unit remains the same and is here assumed to be the same as for one micro BS. Hence, the same power model as for one micro BS can be applied to one DAS cell.

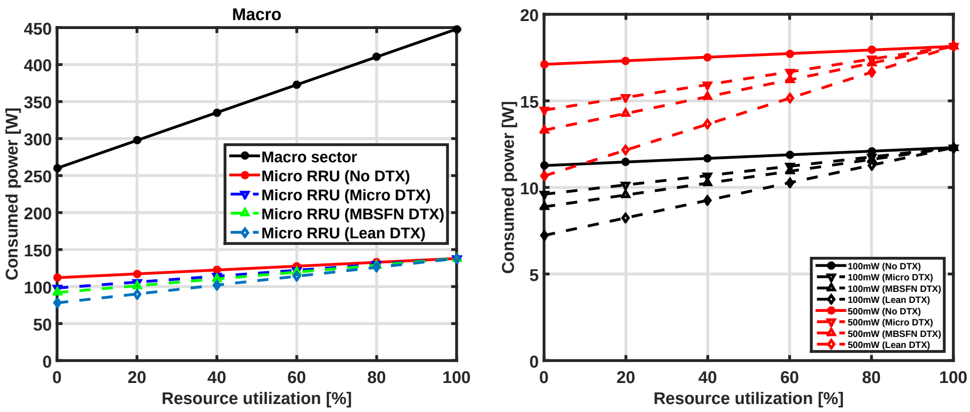

(a) Macro and micro RRU

(b) Pico

Figure 5.8: Power models used in simulations. (a) show power consumption per macro sector and micro RRU. (b) show power consumption of pico nodes with 100mW and 500mW transmit power.

The simulations of longer sleeping periods were carried out as well. The steps for such a simulation are the following:

- First the HetNet deployment is simulated with all small cells switched on. This simulation is performed to find out which small cell each user is connected to.
- Then one simulation of the macro reference depolyment is performed over the considered load range. This is done for estimating the performance for the users in the small cell buildings for different loads.
- Based on the performance of the users in each small cell, a decision is made on whether to switch on the small cell or not. The decision rule, which is based on two thresholds, was found by experimentation. The first threshold is whether the bitrate on any link in from a macro to a user in the small cell goes below 12 Mbps. The other threshold is based on the utilization of the macro sectors covering the users in the small cell. The

small cell is switched on if any of these macro sectors have a utilization above 20% and the bitrate threshold is passed.

Chapter 6

Simulation Results

6.1 Energy efficiency without energy savings

6.1.1 Sparse Pico Deployment

The energy performance of the sparse pico deployment for varying system throughputs can be seen in Figure 6.1 with power per area unit in Figure 6.1(a) and energy per bit in Figure 6.1(b). Power per area unit is calculated over the the 1 km^2 central area described in Subsection 5.4. The contribution from each serving node to the power per area unit is calculated by normalizing the total power by the fraction of utilization generated from the users inside the central area.

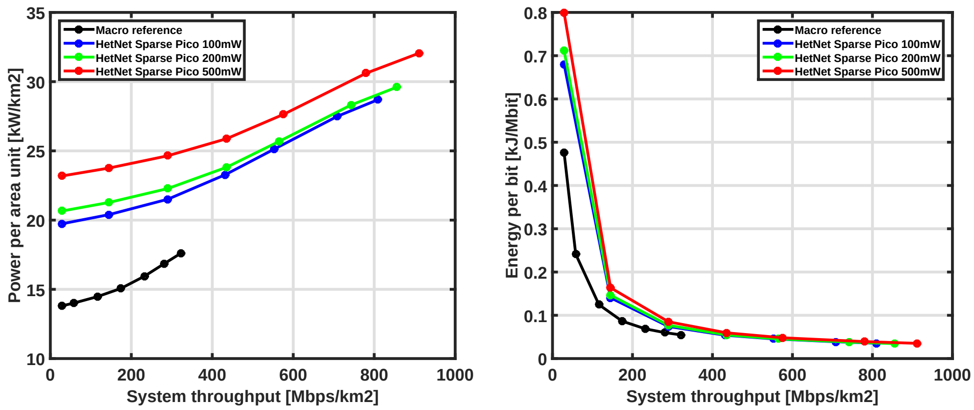

(a) Power per area unit

(b) Energy per bit

Figure 6.1: Energy performance of sparse pico HetNet for different pico Tx powers.

The HetNet simulations were performed with 100mW, 200mW and 500mW transmit power in the pico nodes. In addition, results from a macro reference are included for comparison. HotZones with 10x traffic were specified in the 10 buildings with small cell deployment both for the HetNet and macro reference simulations.

From Figure 6.1 we can conclude that power per area unit increase with higher system throughputs, and observe that the energy per bit quantity have the opposite behavior. This is because the served traffic, i.e. system throughput, increases faster than the power consumption. The highest energy per bit is therefore at low system throughput which illustrates that the energy efficiency is poor in low load situations.

We can also conclude that both power per area unit and energy per bit is higher for the HetNet deployments than the macro reference. To understand the reason for this we can look at the contribution from the macro and small cell layer individually, depicted in Figure 6.2.

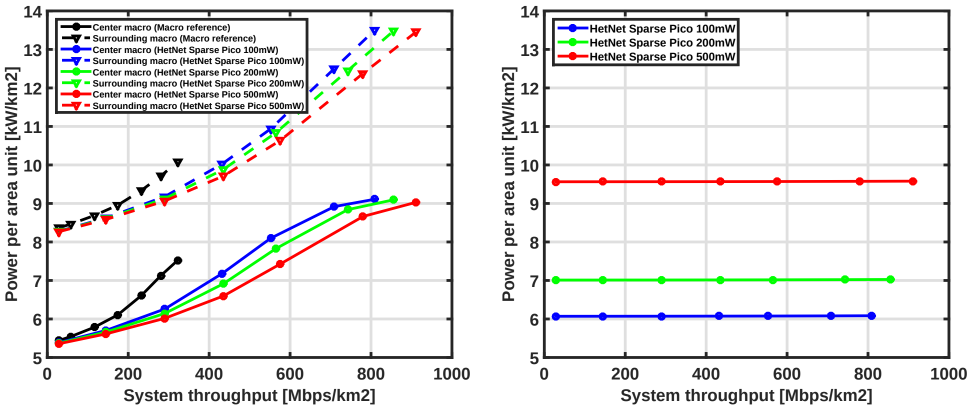

(a) Contribution from macro layers.

(b) Contribution from pico layer

Figure 6.2: Contribution from macro and sparse pico deployment to total power consumption.

In Figure 6.2(a) we see the contribution to the power per area unit from the center and surrounding macro deployments. There we see that with the HetNet configurations the contribution from macro is reduced, which is an offloading effect on the macro utilization from deploying the pico cells. Increasing the transmit power of the pico cells increase the offload since the range of the small cell BSs increase and thus, more users can be offloaded from the macro. However, as Figure 6.2(b) illustrates, the power consumed by the pico layer is quite high, e.g. 500mW pico layer consumes more power than both of the macro layers at low loads. Additionally, we see that the power consumption is almost constant over all system throughputs due to the low load dependency in the pico power model. All these observations leads to the conclusion that the offloading cannot compensate for the additional power added from the pico cells, and hence the total power per area unit is increased.

The offloading of users from the macro layer to the pico layer also affects the QoS experienced by the users. As a measure of this we look at the DL user throughput which is represented by a cumulative distribution function in the simulator. To get relevant measures we look at the 10^{th}, 50^{th} and 95^{th} percentile of this distribution. The 10^{th} percentile will represent the perceived experience of the cell edge users, i.e. worst users. The 50^{th} percentile represent the median user experience and the 95^{th} percentile represents the peak rates, i.e. best users. The QoS results from the sparse pico deployment can be seen in Figure 6.3.

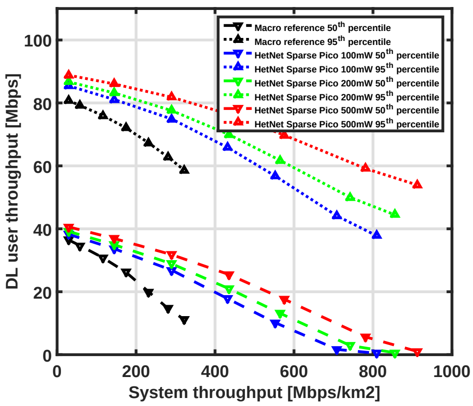

(a) 50^{th} and 95^{th} percentile

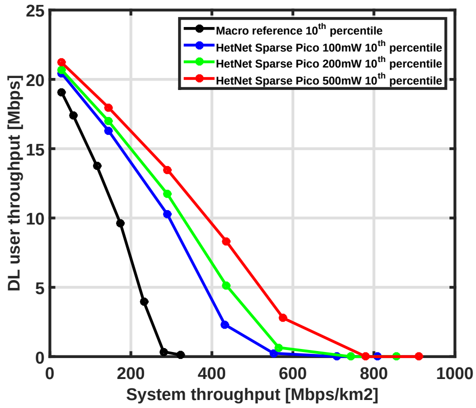

(b) 10^{th} percentile

Figure 6.3: User experience in sparse pico HetNet for different pico Tx powers.

Looking at the median and peak rates in Figure 6.3(a) and the cell edge user rates in Figure 6.3(b) we see that introducing the pico nodes increases the rates experienced by the users. Increasing the transmit power of the pico cells also increases the rates, again since the range of the pico cells is increased which allows more users to be offloaded from the macro. When the cell edge user rates drop to zero the network is getting overloaded, i.e. traffic demand is so high that some users will get no data at all. In Figure 6.3(b) we see that the macro reference network is getting overloaded quicker than the HetNet deployments, or in other words, the capacity of the HetNets is higher than the macro reference. We also see that increasing the transmit power of the pico nodes increases the capacity. Increasing the simulated traffic demand, i.e. offered traffic, when the network is overloaded does not increase the system throughput since no more traffic can be served. This explains why the graphs corresponding to the macro reference network ends at lower system throughputs than the HetNet graphs.

6.1.2 Dense Pico Deployment

Considering the dense deployment of pico nodes with the same variation of transmit powers as in Subsection 6.1.1 we see similar behaviour. Again power per area unit and energy per bit is higher than the macro reference which can be seen in Figure 6.4.

As can be seen in Figure 6.5(a), the offloading of the macro power is similar to that of the sparse deployment, however the effect of tuning the output power of the pico nodes is smaller than in the sparse deployment. A reason for this could be that the indoor dominance of the dense pico deployment is high, even with low transmit power. So increasing the transmit power have a smaller effect on the indoor coverage.

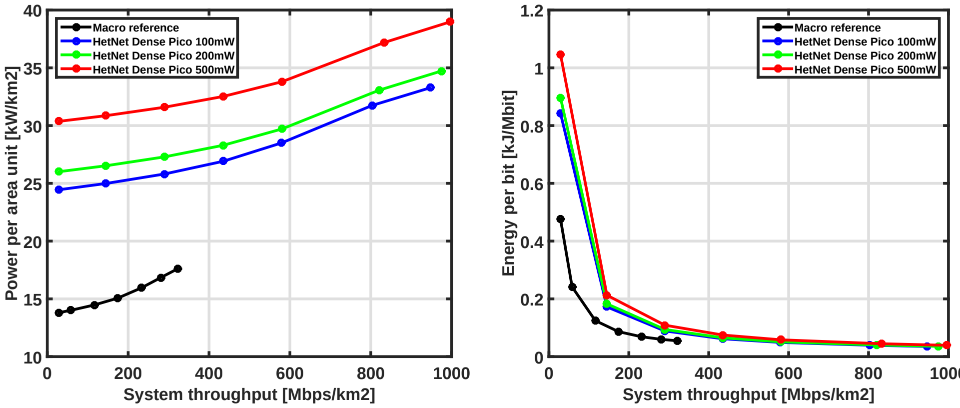

(a) Power per area unit

(b) Energy per bit

Figure 6.4: Energy performance of dense pico HetNet for different pico Tx powers.

In Figure 6.5(b) we can see that the addition of power from the pico layer show similar behaviour as the sparse deployment. However, the additional power is higher than that of the sparse deployment because the number of nodes deployed is higher.

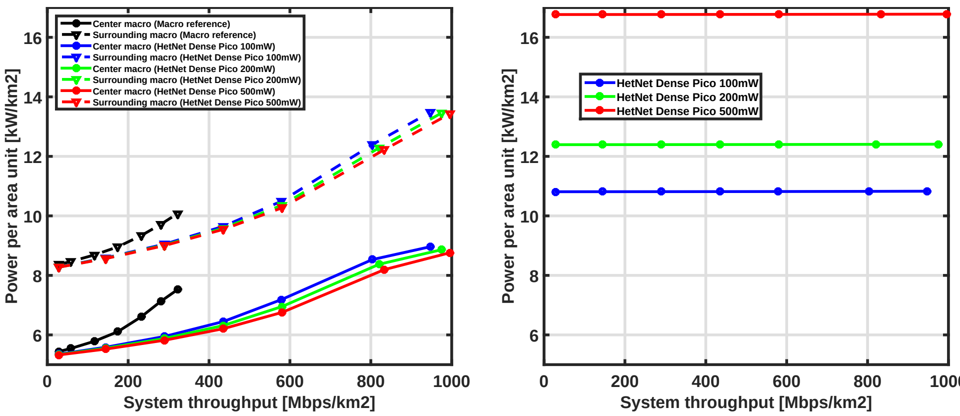

(a) Contribution from macro layers.

(b) Contribution from pico layer

Figure 6.5: Contribution from macro and dense pico deployment to total power consumption.

Regarding user experience we can see that we have the same behavior as in the sparse deployment in Figure 6.6, but as with the offload on the macro layer, tuning the output power of the pico cells have smaller effect on the cell edge user performance.

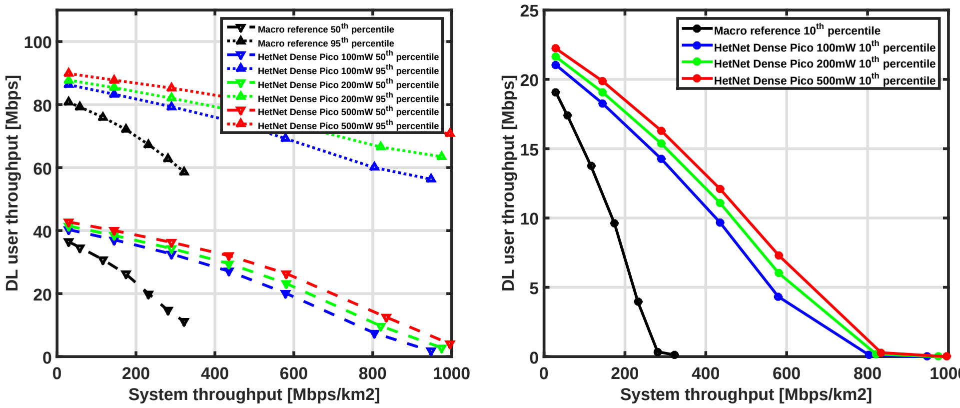

(a) 50th and 95th percentile

(b) 10th percentile

Figure 6.6: User experience in dense pico HetNet for different pico Tx powers.

6.1.3 Micro DAS Deployment

Here follow the simulation results with the micro DAS deployed in the small cell buildings. For this deployment the dense placement of transmission points was used. The power per area unit and energy per bit for these deployments compared to the macro reference is depicted in Figure 6.7 .

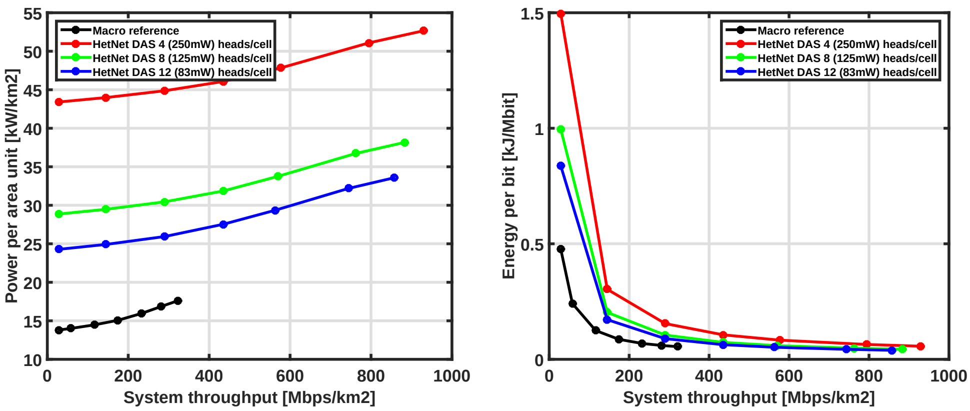

(a) Power per area unit

(b) Energy per bit

Figure 6.7: Energy performance of sparse pico HetNet for different pico Tx powers.

Instead of varying the output power as in previous section, we here vary the number of antenna heads per DAS cell. This is however indirectly effecting the output power since higher number of antenna heads with a constant RRU output power results in lower output power from each antenna head. With 4, 8 and 12 antenna heads per cell, the resulting output power per antenna head is 250mW, 125 mW and 83 mW respectively.

Figure 6.8 show the contribution from the macro and small cell layers and we can there see that the power consumption in the DAS layer is high compared to the macro layer. In Figure 6.8(b) we see that the fewer antenna heads per cell, the higher total power consumption. This is because the number of transmission points is kept constant, so fewer antenna head per cell require more micro RRUs which results in higher total power consumption.

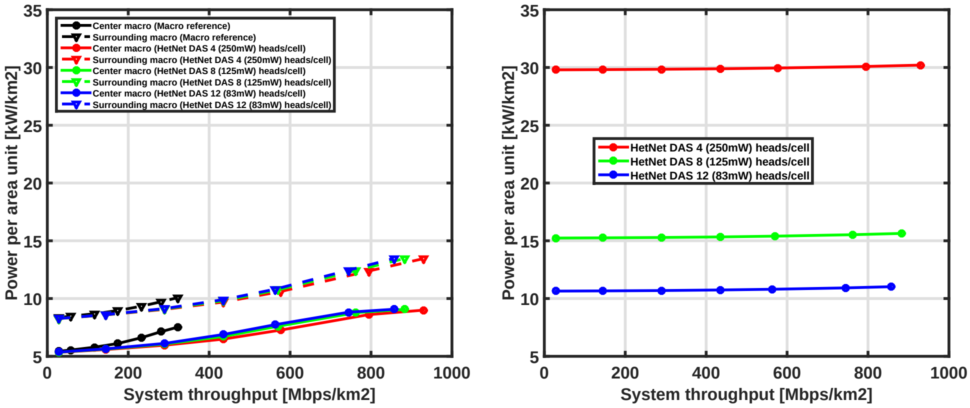

(a) Contribution from macro layers.

(b) Contribution from micro DAS layer

Figure 6.8: Contribution from macro and pico layer to total power consumption per area unit.

Finally we see the user experience of the micro DAS deployment in Figure 6.9.

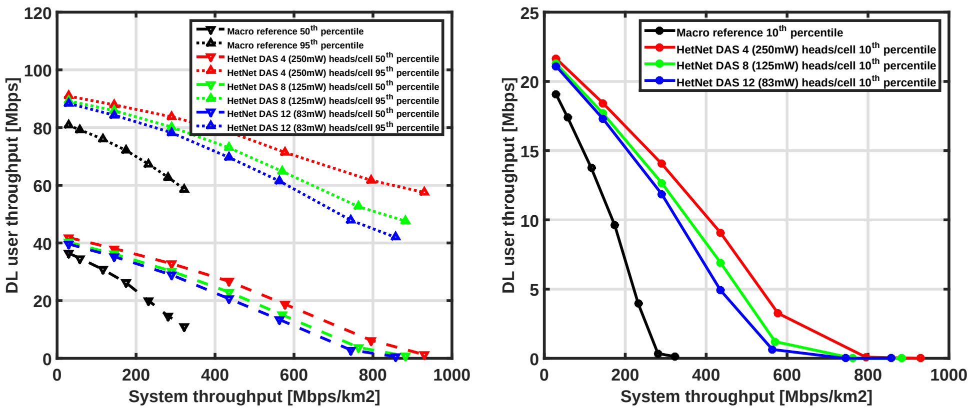

(a) 50^{th} and 95^{th} percentile

(b) 10^{th} percentile

Figure 6.9: User experience in micro DAS HetNet for different number of antenna head per cell.

6.1.4 Effect of HotZones

As mentioned earlier, the previous simulations were performed with 10x traffic HotZones in the buildings with small cell deployments. It is however important to investigate the effect of these HotZones by comparing the results with simulation without HotZones. Figure 6.10 show the effect of HotZones on the the sparse 500mW pico HetNet and the macro reference with power per area unit in Figure 6.10(a) and 10$^{\text{th}}$ percentile DL user throughput in Figure 6.10(b).

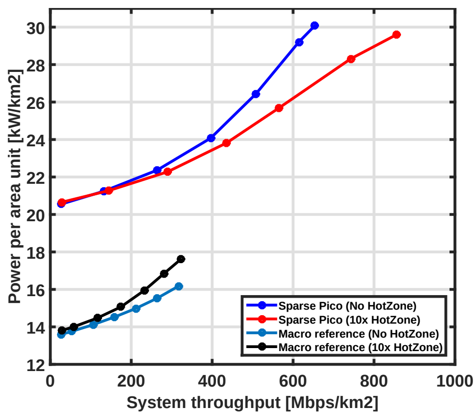

(a) Power per area unit

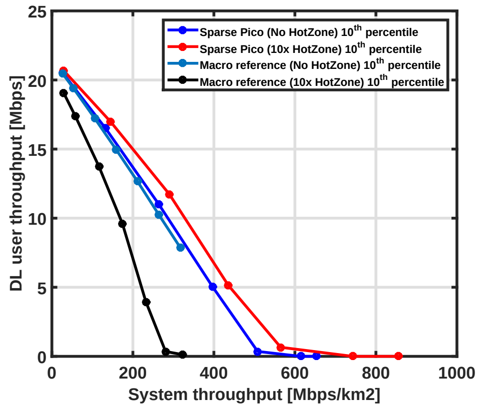

(b) 10$^{\text{th}}$ percentile DL user throguhput

Figure 6.10: Performance of sleep modes in 500mW Pico HetNet..

As can be seen in Figure 6.10(b), introducing traffic HotZones make the macro reference network overload more quickly. In Figure 6.10(a) we also see that the power consumption of the macro reference increases quicker with the HotZones introduced. An interesting detail is however that the HetNet show the opposite behavior. This is because the HotZones are introduced in the buildings with small cell deployment, allowing the small cells to offload more traffic from the macro layer. If the HotZones would have been specified in other locations than the buildings with small cell deployment, the results would have looked more similar to the macro reference results.

This shows how important the choice of sites for small cell deployment is, both for good energy performance and user experience. Deployment of small cells in areas where the demand for capacity is low adds extra power consumption without any performance benefits.

6.1.5 Comparison and Analysis

The previous subsections presented the effect of deploying various indoor small cells compared to having only macro sites covering the area. We can from these sections conclude that from an user experience perspective, the macro only deployment perform worse than all of the small cell deployments. However, the power consumption of the HetNets is generally higher than the macro reference. In this section we will compare the energy performance and user experience in the different HetNet deployments.

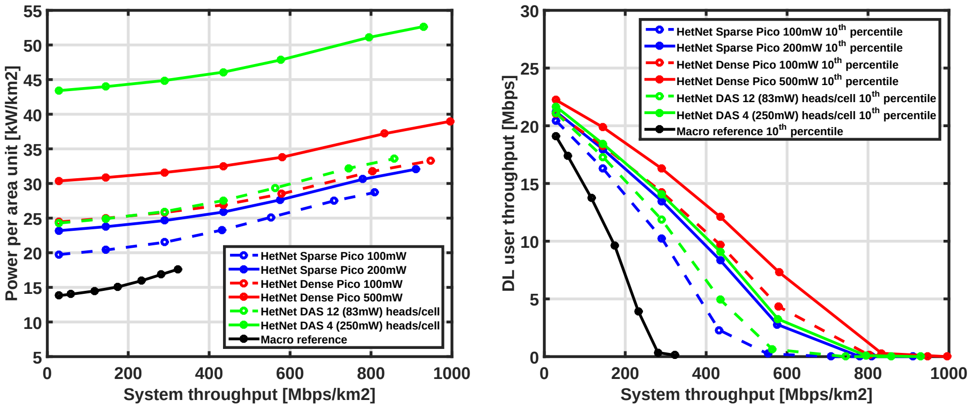

(a) Power per area unit (b) 10^{th} percentile DL user throguhput

Figure 6.11: Comparison of HetNet deployments.

Figure 6.11 show the performance of a subset of the considered HetNets with power per area unit in Figure 6.11(a) and 10^{th} percentile DL user throughput in Figure 6.11(b).

In Figure 6.11(a) we see that the micro DAS with 4 antenna heads per cell have the highest power consumption per area unit. Additionally we see that the sparse 100mW pico deployment have the lowest power consumption out of the HetNets. Dense 100mW pico, sparse 500mW pico and micro DAS with 12 antenna heads per cell have almost the same power consumption.

As a strict definition of the capacity we use the system throughput for which the 10th percentile user throughput in Figure 6.11(b) drops bellow 10 Mbps. In Table 6.1 we see the system capacity of the different HetNet deployments according to this definition. We can here conclude that out of the HetNets, the dense 500mW pico deployment have the highest capacity and the sparse 100mW pico deployment have the lowest capacity. Sparse 500mW pico, dense 100mW pico and micro DAS with 4 antenna heads per cell have almost the same capacity.

Table 6.1: System capacity of HetNet deployments.

Network	Capacity [Mbps/km^2]
Dense Pico 500mW	499
Dense Pico 100mW	425
Micro DAS 4 heads/cell	408
Sparse Pico 500mW	388
Micro DAS 12 heads/cell	329
Sparse Pico 100mW	295
Macro reference	168

To illustrate the tradeoff between user experience and energy performance, Figure 6.12 show the energy per bit on the vertical axis and 10th percentile user throughput on the horizontal axis. For a specified system throughput every HetNet deployment results in a specific point in this plane. To compare energy efficiency at low and high loads, results in Figure 6.12(a) and Figure 6.12(b) are from simulations with system thoughputs of 50 Mbps/km^2 and 400 Mbps/km^2 respectively.

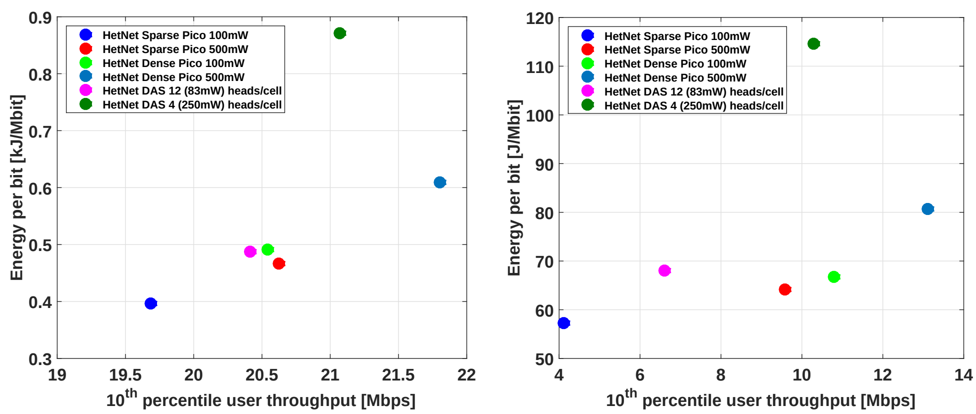

(a) Low system throughput of 50 Mbps/km^2 (b) High system throughput of 400 Mbps/km^2

Figure 6.12: Energy efficiency plot for comparing deployments. Horisontal axis show performance and vertical axis show energy performance in terms of energy per bit.

Firstly, these two plots show that the energy per bit is much higher at low loads for all deployments (note the difference in units with kJ/Mbit in Figure 6.12(a) and J/Mbit in Figure 6.12(b). This is excpected since the total served traffic is very low at low loads, and the energy per bit therefore increases.

In Figure 6.12(a), we again see that dense 100mW pico, sparse 500mW pico and DAS with 12 antenna heads per cell show have similar energy efficiency at low loads. But at higher system throughputs they differ more as can be seen in Figure 6.12(b), where the dense 100mW pico show better cell edge performance but still similar energy performance as the other two.

Apart from the micro DAS with 4 antenna heads per cell, we see a close to linear relationship between energy performance and cell edge user throughput, starting from sparse 100mW pico with low DL throughput and low energy consumption, and ending at dense 500mW pico with high DL performance and high energy consumption. This shows that increasing QoS in a HetNet increase energy consumption if no energy saving techniques are introduced.

The exception from this conclusion is the micro DAS with 4 antenna heads per cell, which have a moderate DL performance compared to its energy consumption. The reason for this is the high number of RRU needed to reach the 250mW transmit power per antenna head. Additionally, feeder losses waste energy fed into the DAS which further reduces the energy efficiency.

6.1.6 Daily Energy Consumption

For comparing the HetNet deployments further, the daily traffic profile described in Subsection 5.3.2 was applied to the simulation results. The daily traffic pattern and power consumption over one day is depicted in Figure 6.13. A peak traffic of 400 Mbps/km^2 was assumed for the HetNets. However, since this is above the capacity of the macro reference, a lower peak traffic of 200 Mbps/km^2 was used for this deployment. Table 6.1 show the deployments with decreasing capacity (the system throughput under which the cell edge users have a user throughput higher than 10 Mbps).

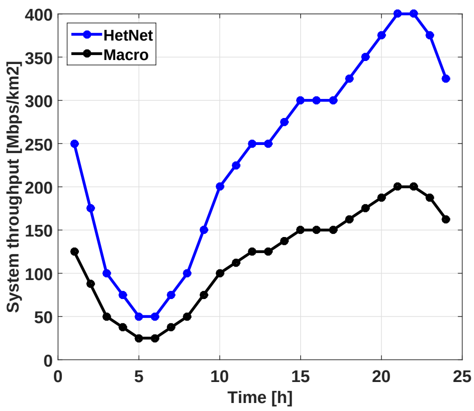

(a) Traffic variation over one day

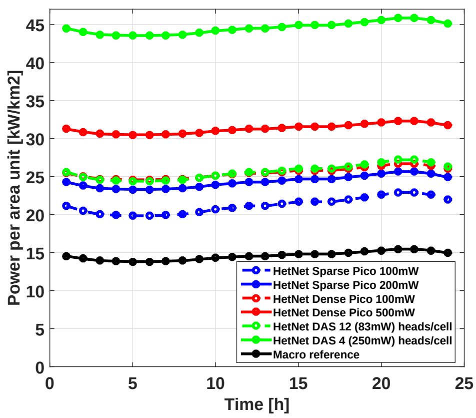

(b) Power consumption over one day.

Figure 6.13: Energy performance of sparse pico HetNet for different pico Tx powers.

6.2 Discontineous Transmission

For assessing the potential energy savings from applying DTX in the small cells, the modified power models described in Section 5.4.3 was applied to the simulation results. A daily traffic profile was applied and the daily energy consumption calculated. As peak traffic for the daily traffic profile, the capacity according to Table 6.1 was used. This means that all the deployments have 10 Mbps cell edge user throughput at the peak hours. The results can be seen in Figure 6.14, where we can see daily energy consumption with no DTX, micro DTX, MBSFN DTX and lean carrier DTX.

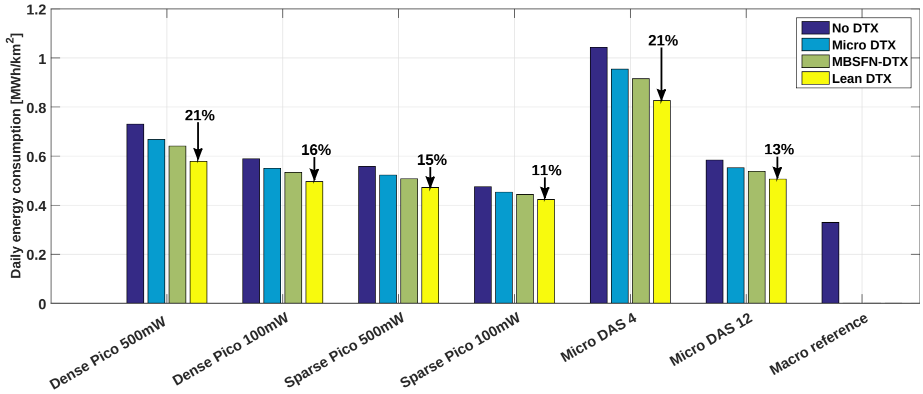

Figure 6.14: DTX energy savings in various HetNet deployments.

From Figure 6.14 we can conclude that the potential for energy savings is the highest in the dense 500mW pico deployment and micro DAS with 4 antenna heads per cell. The reason for this is that the average utilization of the small cell layer is smaller in these deployments. Lower utilization of each node makes higher possibility for DTX energy savings. To get a substantial decrease in total energy consumption the small cells have to constitute a high portion of the total power consumption while at the same time having a low average utilization. This is true for both dense 500mW pico and micro DAS with 4 antenna heads per cell which is why they benefit the most from DTX.

6.3 Small Cell Sleep Modes

Longer sleep modes was simulated for the sparse 500mW and dense 100mW pico HetNets. In Figure 6.15 the performance of the sparse 500mW pico HetNet with sleep modes applied is depicted.

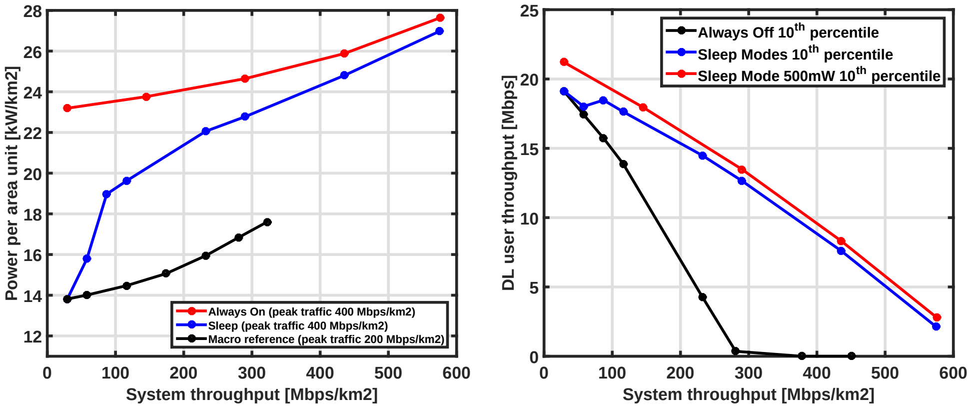

(a) Power per area unit (b) 10^{th} percentile DL user throguhput

Figure 6.15: Performance of sleep modes in 500mW Pico HetNet..

In Figure 6.15(a) we can see that the power consumption of the HetNet with sleep enabled (referred to as “Sleep” in the figure legend) is reduced by applying the sleep modes. At the lowest load the power consumption is the same as for the macro reference since all small cells are switched off. With increasing load, more small cells are switched on which makes the power consumption approach the power consumption of the HetNet with all small cells switched on (referred to as “Always On” in the legend).

As the energy consumption is reduced from introducing small cell sleep modes, the user experience is affected as well. This can be seen in Figure 6.15(b) where the 10^{th} percentile user throughput for the sparse 500mW pico HetNet with and without sleep modes is shown together with the macro reference. At low loads, the performance of the sleep enabled HetNet is the same as the macro reference, again since almost all small cells are switched off. And as with the power per area unit, the sleep enabled HetNet approaches the “Always On” HetNet for higher system throughputs. So the reduced energy consumption comes at a cost of a slight degradation in cell edge user performance, especially at low loads.

The number of small cells switched on for each load level can be seen in Figure 6.16(a).Additionally, the simulation results was mapped to a daily power consumption profile to illustrate the behavior of the sleep modes over one day. 400 Mbps/km^2 was used as peak traffic demand. The result can be seen in Figure 6.16(b). In this figure we can see that its mainly during the periods of low traffic that the sleep modes can save energy, e.g. during the period of lowest traffic the sleep mode save 33% of the power per area unit.

The daily energy consumption with and without sleep modes was calculated for both the sparse 500mW and dense 100mW pico HetNets.The results with energy savings in percent can be seen in Figure 6.17. In addition to the small

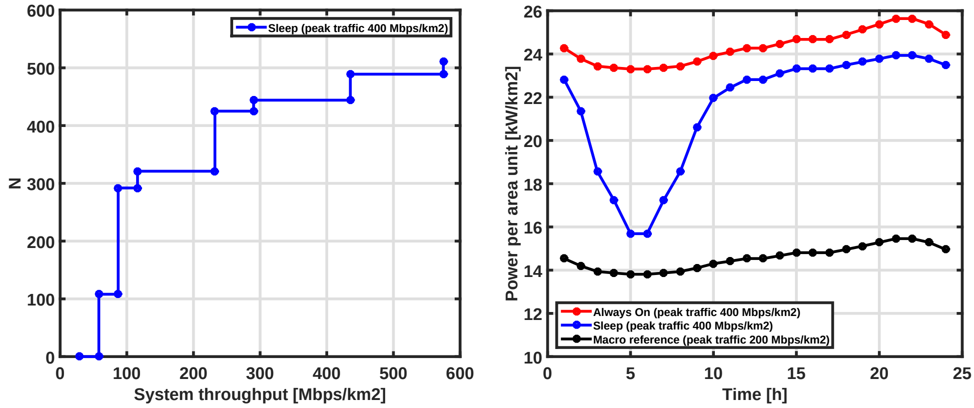

(a) Number of small cells on at different loads.

(b) Daily power consumption

Figure 6.16: Illustration of how small cells are switched on for higher loads and savings in daily power consumption in sparse 500mW pico HetNet.

cell sleep modes, cell DTX can be applied to the small cells that are switched on. The setup of small cell sleep modes with lean carrier DTX is therefore also included in Figure 6.17. We can see that the percentual energy savings is slightly higher in the sparse 500mW HetNets. But we must also remember that the capacity of the dense 100mW is higher than the sparse 500mW.

Compared to the macro reference the pico HetNets has around 75% higher daily energy consumption without energy savings. However, with sleep modes and lean carrier DTX, this can be reduced to only 30% higher than the macro reference.

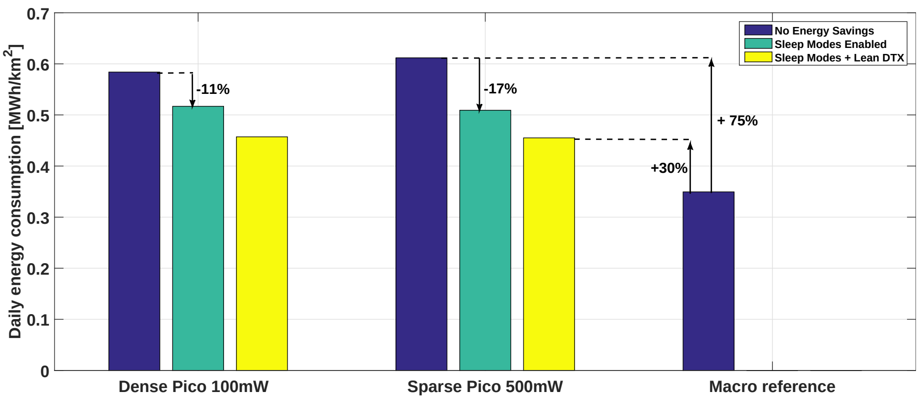

Figure 6.17: Energy savings from sleep modes in pico HetNets.

Chapter 7

Conclusions and Future Work

In this report, the energy efficiency of LTE HetNets have been investigated. Simulations have been carried out for HetNets consisting of a macro network complemented with small cells deployed in the 10 largest building and the HetNets are compared to a macro only reference. The considered small cells are pico with various transmit powers and two different micro DAS. The results show that the deployment of small cells increase the performance of the network, but without energy saving techniques the power consumption of the HetNet deployments is up to 3x higher than that of the macro reference. However, with energy saving techniques such as DTX and small cell sleep modes, the energy consumption of the HetNets can be reduced.

Deployment of HetNets is a tradeoff between energy consumption and performance. As the results shows, the capacity and user experience in a dense urban LTE network can be improved by deploying indoor small cells. Both due to increased performance in the small cell areas as well as due to offloading of the covering macro network. But the trend of the results is that higher performance comes at a price of higher energy consumption. For example, a dense high-power pico deployment have a capacity of around 3x the macro reference but also a daily energy consumption almost 2x the macro reference.

According to the results, a dense low power pico deployment is hard to separate from a sparse high power pico deployment. So from this work, the conclusion is that from an energy performance perspective, they are equally efficient. Micro DAS however, have shown to be a deployment of poor energy efficiency due to high feeder losses in the cables.

The power per area unit in the studied HetNets, including the macro only reference, is higher compared to the simulation results from the dense urban scenario in EARTH [3]. The main reason for this is that the system throughput in the simulations in this thesis is higher compared to the dense urban scenario in the EARTH project, e.g up to 400 Mbps/km^2 compared to the peak area throughput of 92 Mbps/km^2 considered in [3]. With the rapid growth of subscriptions and demand for traffic in mind, we find it justified to study the behavior of HetNets in such situations of higher traffic demand.

We have also seen that the offloading effect the small cells have on the macro network is more apparent if there are traffic HotZones in the areas with small cell deployment.The HetNets actually consume less energy when there is a traffic HotZone in the small cell area than if there is none. This leads to the conclusion that the energy efficiency of a HetNet greatly depends on the choice of location for small cell deployment.

Regarding savings from DTX, we have concluded that the amount of savings is related to the utilization and amount of power consumption in the small cells. Therefore, a dense deployment with good indoor coverage makes higher potential for energy savings. The results also show that the total daily energy consumption of the HetNets can be reduced by 10-20% with lean carrier DTX.

Introducing longer sleep periods also show potential for energy savings. The result shows that with a sparse pico deployment, the power consumption at low traffic loads can be reduced by 33%. Furthermore, we have shown that the energy consumption of the network over one day can be reduced by 17% with a dense pico deployment with only a small degradation compared to having the small cells on all the time. Longer sleep modes combined with DTX therefor show great potential for reducing the power consumption of a HetNet.

Previous studies of energy saving techniques have shown that HetNet energy consumption can be reduced to lower than the macro only network. For example in [9], were the HetNets enabled with DTX and long term sleep modes under some conditions are more energy efficient than the macro reference. In this thesis however, we have found that all the HetNets consume more energy than the macro reference. The total consumption of the small cells as well as the amount of savings that sleep modes can achieve both greatly depends on the deployment scenario. As have been seen in this thesis, the number of small cells, their transmit power and node placement affects both user experience and energy consumption. There may very well be other HetNet deployment scenarios that show good performance, while the total energy consumption with energy saving techniques enabled is lower than the macro reference. However, since the results in this study has not been able to find such a deployment, this is left as a question for future studies.

In this study, we have considered very explicit dense urban environment in the simulations. Also, only the 10 largest buildings were chosen for small cell deployment. The limiting factor has been the time consuming calculations of the matrix containing the gain between the nodes in the simulated network. However, in future studies one could consider a number of other scenarios. For example deployment of small cells in another subset of buildings e.g. the buildings with weakest received signal power from the macro. Also, other choices for placement inside the buildings could be investigated. Furthermore, similar studies could be made for other types of cities could be carried out. The simulation framework contains similar city models of American and European cities. Finally, other types of areas such as rural and urban could be studied from an energy perspective to get an idea of the energy consumption of an entire LTE network.

Regarding propagation models, there might exist more appropriate models for indoor propagation than BEZT. Also, to make the results more realistic, one could run simulations with indoor floor-plans consisting of rooms and hallways etc.

Static simulations is an effective method for estimating the potential for energy savings in a certain deployment, however these types of simulations have limitations in terms of understanding the dynamical behavior of various sleep mode algorithms. For example, a dynamical simulator would be necessary to find out how users are affected by DTX in terms of latency. Furthermore, a dynamical simulator could more realistically model the small cell sleep modes, for example simulating a low power sniffer detecting users entering the small cell.

Bibliography

[1] Earth project web-site. `https://www.ict-earth.eu/`. Accessed: 2015-05-27.

[2] Energy efficiency analysis of the reference systems, areas of improvements and target breakdown. *EARTH Deliverable 2.3*, 2010.

[3] Final integrated concept. *EARTH Deliverable 6.4*, 2010.

[4] Green radio technologies. *EARTH Deliverable 4.2*, 2010.

[5] Heterogeneous networks - securing excellent mobile broadband user experience, everywhere. *Ericsson White Paper*, 2014.

[6] G. Auer, V. Giannini, C. Desset, I. Godor, P. Skillermark, M. Olsson, M.A. Imran, D. Sabella, M.J. Gonzalez, O. Blume, and A. Fehske. How much energy is needed to run a wireless network? *Wireless Communications, IEEE*, 18(5):40–49, October 2011.

[7] Jung-Fu Cheng, H. Koorapaty, P. Frenger, D. Larsson, and S. Falahati. Energy efficiency performance of lte dynamic base station downlink dtx operation. In *Vehicular Technology Conference (VTC Spring), 2014 IEEE 79th*, pages 1–5, May 2014.

[8] A. Damnjanovic, J. Montojo, Yongbin Wei, Tingfang Ji, Tao Luo, M. Vajapeyam, Taesang Yoo, Osok Song, and D. Malladi. A survey on 3gpp heterogeneous networks. *Wireless Communications, IEEE*, 18(3):10–21, June 2011.

[9] Laetitia Falconetti, Pal Frenger, Harald Kallin, and Thomas Rimhagen. Energy efficiency in heterogeneous networks. In *Online Conference on Green Communications (GreenCom), 2012 IEEE*, pages 98–103, Sept 2012.

[10] Mikael Fallgren, Magnus Olsson, and Per Skillermark. Energy saving techniques for lte: Integration and system level results. In *Personal Indoor and Mobile Radio Communications (PIMRC), 2013 IEEE 24th International Symposium on*, pages 3269–3273, Sept 2013.

[11] A. Fehske, G. Fettweis, J. Malmodin, and G. Biczok. The global footprint of mobile communications: The ecological and economic perspective. *Communications Magazine, IEEE*, 49(8):55–62, August 2011.

[12] P. Frenger, P. Moberg, J. Malmodin, Y. Jading, and I. Godor. Reducing energy consumption in lte with cell dtx. In *Vehicular Technology Conference (VTC Spring), 2011 IEEE 73rd*, pages 1–5, May 2011.

[13] C. Hoymann, D. Larsson, H. Koorapaty, and Jung-Fu Cheng. A lean carrier for lte. *Communications Magazine, IEEE*, 51(2):74–80, February 2013.

[14] M. Kurras, K. Borner, L. Thiele, M. Olbrich, and T. Haustein. Achievable system performance gains using distributed antenna deployments. In *Personal Indoor and Mobile Radio Communications (PIMRC), 2012 IEEE 23rd International Symposium on*, pages 143–148, Sept 2012.

[15] Ben Slimane Lars Ahlin, Jens Zander. *Principles of Wireless Communications*. Studentlitteratur, 2006.

[16] M. Mihaylov, A. Mihovska, R. Prasad, P. Semov, and V. Poulkov. Energy efficiency vs. throughput trade-off in an lte-a scenario. In *Wireless Communications, Vehicular Technology, Information Theory and Aerospace Electronic Systems (VITAE), 2014 4th International Conference on*, pages 1–5, May 2014.

[17] David Lister Tim Oï£¡Farrell Walter Tuttlebee, Simon Fletcher and John Thompson. Saving the planet ï£¡ the rationale, realities & research of green radio. *ITP Journal Paper*, June 2010.

[18] S. Yunas, M. Valkama, and J. NiemelaÌĹ. Spectral and energy efficiency of ultra-dense networks under different deployment strategies. *Communications Magazine, IEEE*, 53(1):90–100, January 2015.